


2019

SPATIOTEMPORAL DYNAMICS OF NITROGEN AND CARBON BIOGEOCHEMISTRY IN A WETLAND- STREAM SEQUENCE

Patrick E. Hurley
University of Montana

Let us know how access to this document benefits you.

Follow this and additional works at: <https://scholarworks.umt.edu/etd>

 Part of the [Applied Statistics Commons](#), [Biogeochemistry Commons](#), [Biology Commons](#), [Environmental Monitoring Commons](#), [Hydrology Commons](#), [Longitudinal Data Analysis and Time Series Commons](#), [Natural Resources Management and Policy Commons](#), [Systems Biology Commons](#), and the [Water Resource Management Commons](#)

Recommended Citation

Hurley, Patrick E., "SPATIOTEMPORAL DYNAMICS OF NITROGEN AND CARBON BIOGEOCHEMISTRY IN A WETLAND-STREAM SEQUENCE" (2019). *Graduate Student Theses, Dissertations, & Professional Papers*. 11357.
<https://scholarworks.umt.edu/etd/11357>

This Thesis is brought to you for free and open access by the Graduate School at ScholarWorks at University of Montana. It has been accepted for inclusion in Graduate Student Theses, Dissertations, & Professional Papers by an authorized administrator of ScholarWorks at University of Montana. For more information, please contact scholarworks@mso.umt.edu.

SPATIOTEMPORAL DYNAMICS OF NITROGEN AND CARBON BIOGEOCHEMISTRY
IN A WETLAND-STREAM SEQUENCE

By

PATRICK EVANS HURLEY

Bachelor of Science, University of Vermont, Burlington, Vermont, 2013

Thesis

Presented in partial fulfillment of the requirements

for the degree of

Master of Science

in Systems Ecology

The University of Montana

Missoula, MT

April 2019

H. Maurice Valett, Chair

Division of Biological Sciences

Marc Peipoch, Co-Chair

Stroud Water Research Center

Benjamin P. Colman

W.A. Franke College of Forestry and Conservation

Spatiotemporal Dynamics of Nitrogen and Carbon Biogeochemistry in a Wetland-Stream Sequence

Chairperson: H. Maurice Valett

Studies of aquatic ecosystems often segregate streams from the influential ponds, lakes, and wetland zones that act as important transitions between terrestrial and fluvial systems. Across the aquatic landscape, these zones interact to form linked ecosystems that function as discrete nutrient processing domains, shifting biogeochemical signals due to spatial and temporal variability in hydrologic and biologic controls. Using a mass-balance approach, we profiled nutrient dynamics along a 23-km wetland-stream sequence over three seasons. Hydrologic, morphologic, and biologic conditions, as well as landscape attributes, were quantified to determine potential controls on biogeochemical cycling in a tributary of the Upper Clark Fork River (UCFR), MT that is known for contributing disproportionate nutrient loads. Results identified a geomorphic and hydrologic sequence of wetland-stream interactions that generated discrete zones of nutrient production, transformation, and uptake. Zones of production resulted in five- to seven-fold increases in nitrate loads. Across all four stream reaches, nutrient dynamics were driven primarily by net groundwater exchange, which explained up to 30% ($P = 0.0064$) of the change in nitrate load. Nitrogen transformation of ammonium-rich groundwater inputs resulted in mean nitrification rates of $248.49 \text{ mg N m}^{-2} \text{ d}^{-1}$; on par with engineered surface-flow constructed treatment wetlands. Abnormally high C loss rates (up to $-54.9 \text{ g C m}^{-2} \text{ d}^{-1}$) calculated from changes in the dissolved organic carbon (DOC) load between ground- and surface water compartments suggest DOC removal pathways other than heterotrophic respiration – i.e., adsorption to the extensive carbonate precipitates which coat benthic and hyporheic substrates. During the study period, water flowing through this sequence of aquatic systems exhibited an average increase in nitrate load of 461% and a doubling of ammonium, soluble reactive phosphate, and DOC loads with a mere 32% increase in discharge.

Acknowledgements

I would like to start by thanking my advisor, H. Maurice Valett, for his endless passion, enthusiasm, and veracity for all things science. The mentorship and friendship throughout the endeavor were critical to the success of this project and my own personal development. I am much more aware of and prepared for the workings of the world because of this experience, and for that I am grateful. I would like to thank Marc Peipoch for his skeptic insight, humor, and thoughtful encouragement each step of the way. To Ben Colman, thank you for your dedication, breadth, and boundless technical expertise. I would like to thank the following members of the Valett, Colman, and DeGrandpre labs at the University of Montana for field and laboratory assistance, moral support, crisis aversion, and associated shenanigans: Kimberly Bray, Fischer Young, Lauren Sullivan, Kaitlin Perkins, Claire Utzman, and Ashley Micklewright. I could not have asked for a finer brigade of swashbuckling scholars to accompany me through this journey. Royce Engstrom brought analytical sanity, guidance, honor, and an impeccable sense of scholarly style (and dress) to the lab, and for that, we are all grateful. The following landowners provided enthusiastic support, enlightening perspectives, and access to their lands that were the focus of this study: Thomas Heggelund; Hans Lambert; Daniel and Donald Ueland; Daniel Kelley. To my family: thank you for your unconditional support while I naively attempt to solve the problems of the world. To my friends, especially A.C.F: thank you for your endless love and encouragement. I am grateful to the folks at the Montana Natural Resource Damage Program for funding and expertise. I would like to acknowledge the Montana Institute on Ecosystems, the Long-Term Research in Environmental Biology program, and the Established Program to Stimulate Competitive Research for promoting scientific investigations that will undoubtedly aid in the enhancement of degraded public resources.

Table of Contents

Acknowledgements.....	iii
Table of Contents.....	iv
List of Tables.....	v
List of Figures.....	v
Appendices.....	vi
1.0 INTRODUCTION.....	1
2.0 METHODS.....	4
2.1 Study Site.....	4
2.2 Biologic and Hydrogeomorphic Structure.....	5
Chlorophyll-a.....	5
Benthic Organic Matter.....	6
Hydrology.....	6
Geomorphology.....	7
2.3 Fixed and Synoptic Sampling.....	7
2.4 Material Loads and Nutrient Processing Rates.....	9
2.5 Data Analysis.....	11
3.0 RESULTS.....	11
3.1 Aquatic Landscape Heterogeneity.....	11
3.3 Spatiotemporal Patterns in Biogeochemistry.....	13
3.4 Nutrient Loads at Main Channel Sites.....	15
3.5 Partitioning ΔL by Hydrology and Biology.....	16
Dissolved Inorganic N.....	16
SRP and DOC.....	18
Biogeochemical Processing of Groundwater Nutrient Loads.....	19
3.6 Rapid Nutrient Processing.....	20
4.0 DISCUSSION.....	21
4.1 Hydro-geomorphic Controls in the LCDC.....	22
Nitrogen Dynamics.....	23
Carbon Dynamics.....	28
4.2 Effects of Management Practices on NPD Character.....	30
5.0 CONCLUSION.....	32
6.0 LITERATURE CITED.....	33

List of Tables

Table 1. Physicochemical, hydrologic, biogeochemical, and biological parameters by reach over the entire study period.....	54
---	----

List of Figures

Figure 1. The Lost Creek Dutchman Complex (LCDC) and designated study reaches.....	55
Figure 2. Landscape attributes of the LCDC.....	56
Figure 3. Net groundwater exchange and groundwater as a proportion of surfacewater input...57	
Figure 4. Nutrient concentrations along a longitudinal gradient during peak and base flow.....58	
Figure 5. Groundwater versus surfacewater nutrient concentrations.....	59
Figure 6. Nutrient loads at each of the five main-channel sites throughout the study period.....	60
Figure 7. Total change in load (ΔL), change in load due to groundwater exchange (ΔL_{gw}), and change in load due to biological processing (ΔL_{bio}) for NO_3^- and NH_4^+ by reach.....	61
Figure 8. Total change in load (ΔL), change in load due to groundwater exchange (ΔL_{gw}), and change in load due to biological processing (ΔL_{bio}) for SRP and DOC by reach.....	62
Figure 9. Total change in nutrient load (ΔL_{bio}) as a function of putative groundwater nutrient loads (ΔL_{gw}) for NO_3^- and DOC.....	63
Figure 10. Area-specific biological processing rates of NO_3^- and DOC by reach.....	64
Figure 11. Comparisons between N and C processing rates in the LCDC with those measured in other aquatic ecosystems.....	65

Appendices

Appendix A. Reach, number, name, description, and location of the ten sampling sites.....	66
Appendix B. Geomorphic parameters and landscape attributes by reach.....	67
Appendix C. Nutrient concentration of each of the dissolved constituents at the five main-channel sites throughout the study period.....	68
Appendix D. Nutrient concentration of each of the dissolved constituents at the five irrigation ditches/tributary inputs throughout the study period.....	69
Appendix E. Loads of each of the dissolved constituents at the five irrigation ditches/tributary inputs throughout the study period.....	70
Appendix F. Total changes in load (L), change in load due to groundwater exchange (L _{gw}), and change in load due to biological processing (L _{bio}) for NO ₃ ⁻ and NH ₄ ⁺ by reach and date.....	71
Appendix G. Total changes in load (L), change in load due to groundwater exchange (L _{gw}), and change in load due to biological processing (L _{bio}) for SRP and DOC by reach and date.....	72
Appendix H. Area-specific biological processing rates of NH ₄ ⁺ and in the LCDC by reach and date.....	73
Appendix I. Uptake length, uptake rate, and uptake velocity for each dissolved nutrient by reach.....	74

1.0 INTRODUCTION

As open ecosystems, rivers and streams play important and unique roles in landscape nutrient budgets because they incorporate both allochthonous and autochthonous sources (Fellows et al. 2006) and have the ability to both transport (Coats and Goldman 2001) and transform (Peterson et al. 2001) nutrients across large spatial scales through linked ecosystems (Vitousek et al. 1979, Kling et al. 2000). Biogeochemical processes are often both a cause and effect of variation in ecosystem structure (Bilby and Likens 1980, Gorham 1991, Fisher et al. 2004), and it is difficult to determine the primary mechanisms that drive biogeochemical variability. Moreover, aquatic ecosystem function is influenced by both ‘local’ and ‘routing’ controls (Valett et al. 2014). Local controls often manifest as heterogeneous habitats with distinct community composition and resulting processes (Kuglerova et al. 2015), whereas routing controls operate through hydrologic linkages that transport energy and materials through various flow paths (Jones et al. 1996). Additionally, many studies have confirmed the existence of spatially-distinct functional domains within streams. For instance, hotspots of denitrification occur in anoxic hyporheic zones and are often only meters in length (Vidon et al. 2010), while emergent spring brooks can be significant contributors of nitrogen (N)-rich groundwater to above-ground channels (Caldwell et al. 2015), likely through mineralization and subsequent nitrification of buried or dissolved organic N (Stelzer 2015).

Nutrient processing in aquatic ecosystems is also driven, in part, by channel morphology (Gücker and Boëchat 2004), hydrologic residence time (Zarnetske et al. 2012), and linkages to the hyporheic zone (Marzadri et al. 2012). Within river networks, these attributes are continually changing due to the shifting habitat mosaic (Stanford et al. 2005), which emphasizes the co-

occurrence of various floodplain habitat types and the feedbacks among them. However, lotic, lentic and wetland systems are often considered independently in scientific investigations because of the very differences in hydrology, geomorphology, and biology that distinguish them. The River Continuum Concept (Vannote et al. 1980) is a well-known model that segregates streams from the influential ponds, lakes, and wetland zones that act as important transitions between terrestrial and aquatic systems (Junk et al. 1989). Conversely, studies of lakes and reservoirs often relegate interconnecting streams to mere conveyors with little internal material processing or integration with the receiving water body (Elser and Kimmel 1985).

At the same time, others have tried to classify spatially discrete zones among linked aquatic ecosystems to better characterize and model various dynamic processes. Ward and Stanford (1983) introduced the serial discontinuity concept as a theoretical perspective to address regulated streams where flow and nutrient dynamics are interrupted by dams, forming a discontinuum of lotic and lentic reaches. Brinson (1993) identified the character of floodplain wetland systems as “donors, conveyors or receptors” based on the role each played in hydrologic budgets and nutrient and sediment exchange. He noted that the source of water and materials to floodplain wetlands, and subsequent processing within, vary with stream order because of influences such as discharge, floodplain width, and floodplain connectivity. Similarly, the Process Domains Concept was put forth as a framework for classifying ecosystem structure and function as products of geomorphic variability and disturbance regimes (Montgomery 1999). This concept generated a discontinuous distribution of systems, the order of which was dictated by large-scale geomorphic settings. More recently, Caldwell et al. (2015) suggested aquatic systems exhibit spatially discrete nutrient processing domains (NPDs), identified by predominant biogeochemical processes that differ in character, magnitude, and efficiency. Such NPDs are

likely distributed through flowing water systems based on routing and local controls (Valett et al. 1996), driven in part by hydrogeomorphic (Doyle et al. 2003), biologic (Martí et al. 1997), and biogeochemical (Ocampo et al. 2006) conditions. A river network characterized by both lotic channels and lentic wetlands in a longitudinal sequence likely exhibits spatially-discrete nutrient processing dynamics. It remains unclear, however, how spatiotemporal, hydrogeomorphic, and biologic heterogeneity result in discrete biogeochemical behavior among a series of linked aquatic ecosystems and their cumulative impact at the watershed scale.

Poole (2002) argued that “fluvial landscape ecology requires the development of tools and techniques that facilitate a discontinuum view of lotic ecosystems”. Unfortunately, the techniques commonly used to assess biogeochemical cycling in streams (i.e., nutrient spiraling, Newbold et al. 1981; tracer injections, Stream Solute Workshop 1990) are often measured at finer scales than those relevant to linked aquatic sequences and are difficult to apply to larger, more heterogeneous landscapes (Peipoch et al. 2016) that include lentic characteristics. While previous studies have addressed the key drivers of nutrient processing in discrete stream reaches (100-1,000 m) (Ensign and Doyle 2006, Hall et al. 2013), here we employ an approach that recognizes key controls over nutrient cycling that are discernible at the landscape scale to better understand biogeochemical dynamics related to linked lotic, lentic, and wetland systems. Moreover, we propose that such an approach lends to tractable assessment of systems and conditions relevant to management concerns and applied priorities.

We asked how biogeochemical processing changes along a wetland-stream sequence and how spatiotemporal patterns characterize nutrient dynamics in linked ecosystems. We posited that along the sequence 1) systems function as discrete nutrient processors due to spatial and temporal variation in hydrologic linkages to surface and subsurface nutrients that control in-

stream biogeochemical cycling, 2) the biogeochemical character of individual reaches will change with time because of the combined influences of seasonal variation in hydrology and biological activity as they relate to nutrient supply, transport, and processing, and 3) biogeochemical function can be differentiated by morphologic and biologic structure because these landscape features shape delivery and processing mechanisms that result in distinct nutrient uptake rates.

We employed a mass-balance approach to address biogeochemical character and assess spatial and temporal variation as it relates to hydrologic, geomorphic, and ecologic conditions in the Lost Creek-Dutchman Complex (LCDC), a wetland-stream tributary of the Upper Clark Fork River (UCFR), MT. The LCDC was an ideal setting to investigate nutrient dynamics, processing controls, and loading rates along a low-order river because of alternating lotic and lentic influences and a 30-year history of disproportionate nutrient contributions to a river undergoing extensive restoration (Ingman and Kerr 1989, Valett and Peipoch 2018). The LCDC provides an opportunity to identify and characterize linkages between discrete NPDs and address how the sequence of reaches influence nutrient dynamics in a heavily-regulated watershed.

2.0 METHODS

2.1 Study Site

Since 1989, the LCDC (46°11'6.24"N 112°49'5.88"W) has been identified as a substantial source of dissolved inorganic N (DIN) to the UCFR, potentially contributing to the occurrence of late-summer nuisance algal blooms in reaches up to 200 km downstream (Ingman and Kerr 1989, Valett and Peipoch 2018). The LCDC is a sequence of linked aquatic ecosystems with over 23 km of stream channel and nearly 1,500 hectares of wetlands (USEPA and CDM Smith 2012) (Figure 1). The aquatic landscape ranges from impounded lentic zones to fast-

moving, incised channels, or highly braided forms with dense riparian cover, while a large peat fen dominates the upper extent of the LCDC. Two perennial streams flow through the complex, Lost Creek and Dutchman Creek, both of which are influenced by groundwater exchange. Lost Creek represents the central lotic axis in the system and originates as a montane stream that enters the complex as a second-order system with baseflow discharge of $\sim 57 \text{ L s}^{-1}$, draining a 157 km^2 catchment (USGS 2018). Dutchman Creek is a smaller springbrook system that originates within the LCDC and converges with Lost Creek along a constructed dyke that generates a substantial open-water component of the larger wetland system. Secondary wastewater treatment ponds located above Dutchman Creek near the top of the LCDC flow into infiltration basins or act as holding ponds for land-application to agricultural fields (Figure 1, MT DEQ 2017).

We performed mass-balance assessments for the LCDC on nine occasions from May to September of 2018. Four study reaches (I-IV) were delineated by five main-channel sites (MC1 – MC5, Figure 1) while five additional sites were used to track irrigation ditches or tributaries, i.e. channelized hydrologic losses or gains to the stream (Appendix A). Reach delineation and water sampling was based on predominant landscape attributes and accessibility for river gaging, a strategy that addressed landscape morphology while considering common limitations associated with tractable watershed management.

2.2 Biologic and Hydrogeomorphic Structure

Chlorophyll-a

Benthic standing stocks were measured as chlorophyll-a (chl-a) and ash-free dry mass (AFDM) during a single baseflow sampling (6 September). We randomly collected five benthic biomass samples from the thalweg at three locations within each reach for chl-a and benthic

organic matter (BOM) analysis. For locations with epilithic biofilm communities, cobbles were scrubbed into a homogeneous slurry and subsampled for chl-a while recording total slurry volume and total scrubbed area. Where macroalgae or macrophytes were dominant, we collected and homogenized biomass from a known area of substrate and recorded wet weight before subsampling. All chl-a samples were extracted in 90% acetone for 24 h in the dark (4°C) and subsequently centrifuged. Absorbance was measured at 430, 664, 665, and 750 nm before and after acidification (0.1N HCl) with a spectrophotometer (Azzota Scientific, Claymont, DE). Absorbance values were converted to chl-a (mg m^{-2}) with corrections for sub-sample volume and sampling area following Steinman et al. (2017).

Benthic Organic Matter

Remaining subsamples from the epilithic or macroalgae/macrophyte biomass collection was used to determine BOM standing stock as AFDM. Subsamples were filtered onto pre-weighed, pre-ashed, glass fiber filters (Whatman PLC, Boston, MA), and dried to a constant weight at 60°C. Samples and filters were then ashed (4 hours, 550°C), wetted, and dried again to a constant weight. BOM stocks (g AFDM m^{-2}) were calculated as the difference between pre- and post-combustion following corrections for total sample volume (or mass) and sampling area. Lastly, we compared chl-a:AFDM ($\text{mg chl-a} : \text{g AFDM}$) to generate an autotrophic index for each individual biomass sample.

Hydrology

Hydrologic residence times, in the form of median travel time, were estimated using conservative tracer techniques following Gordon et al. (1992). This approach was applied to each reach on at least three occasions over the course of the study, and linear relationships with stream discharge generated to address residence time across the study period. Due to the lentic extent of Reach I, we derived residence times by coupling conservative tracer measurements of the

flowing stream channel and estimated residence time for the lentic water body. At peak and base flow, we estimated lentic water body volume using aerial imagery and 12 transects of equally-spaced depth measurements. Thus, volume (L) was divided by hydrologic discharge (Q ; $L \text{ sec}^{-1}$) at the outflows to estimate residence times. Total residence times for Reach I were the sum of estimated times for the lotic and lentic portions. Between mid-July and late August, a diversion dam removed the majority of channel water near the top of Reach III. During that time period, we measured residence time for the residual channel water below the diversion dam as it flowed towards Reach IV.

Geomorphology

Geomorphic measurements used to assess channel, floodplain, and wetland morphology were taken over a two-week period during the receding limb of the hydrograph (early July 2018). Metrics were those commonly used for floodplain and stream assessments. A minimum of 12 randomly located transects were used to measure bankfull width, channel width:depth ratio, cross-sectional area, incision ratio, maximum bankfull depth, mean bankfull depth, pool width:depth ratio, riffle:run ratio, sinuosity, and substrate size as defined in Rosgen (1994). We estimated primary land cover types (upland, wetland, open water) for each reach using publically-available habitat mapping products (MT NHP 2018) and open-source geographic information systems (QGIS Development Team 2019). Whole reach bed area (km^2) estimations included wetted area of the stream channels, lentic zones, and perennial flow-through wetlands. Floodplain wetlands that were not clearly inundated and connected to the stream channel were not included in whole reach bed area estimates.

2.3 Fixed and Synoptic Sampling

Physicochemical conditions, hydrologic discharge, and dissolved nutrient concentrations were measured biweekly from May to September 2018 at all 10 sites. Physicochemical measures

including temperature ($^{\circ}\text{C}$), specific electrical conductivity ($\mu\text{S cm}^{-1}$), dissolved oxygen (DO; mg L^{-1} and % saturation), and pH were measured using handheld probes (YSI Model 2030, Yellow Springs, OH). Discharge was measured by two USGS gage stations (#12323850 and #12323840, Reston, VA), a handheld acoustic Doppler velocimeter employing the area-velocity approach (SonTek, San Diego, CA), and by using conservative tracer dilution gaging (Gordon et al. 1992) to quantify flow in the main channel, contributing inputs, and irrigation withdrawals. Measurements of dissolved nutrient concentrations included nitrate-N ($\text{NO}_3\text{-N}$; mg L^{-1}), ammonium-N ($\text{NH}_4\text{-N}$, mg L^{-1}), soluble reactive phosphorus (SRP; mg L^{-1}), and dissolved organic carbon (DOC; mg L^{-1}).

High-resolution (~ 0.5 km) synoptic surface water sampling of the 23-km sequence occurred during peak (6 June) and base (22 August) flow conditions. Collection of samples (June, $n=41$; August, $n=43$) occurred during mid-day over a 3-hour span. During late summer, 19 screened groundwater wells (Atlantic Supply, Orlando, FL) were installed along the LCDC sequence. All wells consisted of 2.5-cm diameter PVC casings with 30-cm slotted screens (slot size, $508\ \mu\text{m}$) inserted 30-50 cm beneath the water table. On 5 September, all wells were emptied and allowed to recharge for ~ 24 hours before being sampled in triplicate by means of a 1.27-cm diameter vinyl bailer.

All water samples for dissolved nutrients were collected in triplicate, except for DOC in groundwater wells ($n = 1$). All water samples were collected and filtered through $0.7\text{-}\mu\text{m}$ glass fiber filters (Whatman PLC, Boston, MA), transported to the laboratory on ice, and frozen (-20°C) until analysis. We measured dissolved $\text{NO}_3\text{-N}$ (as nitrate + nitrite), $\text{NH}_4\text{-N}$, and SRP on a segmented-flow analyzer (Astoria-Pacific AP2, Clackamas, OR). Nitrate was assessed using the cadmium reduction method and absorbance measured at 540 nm (U.S. EPA 1993d). Ammonium

was analyzed following the phenol-hypochlorite method and absorbance measured at 660 nm (U.S. EPA 1993b). SRP was determined according to the ascorbic acid method and absorbance measured at 700 nm (U.S. EPA 1993c). DOC was analyzed using heated persulfate digestion (U.S. EPA 2005) on a total carbon analyzer (OI Aurora 1030W, College Station, TX).

2.4 Material Loads and Nutrient Processing Rates

We performed hydrologic and material mass-balances for the four delineated reaches on nine sampling dates between May and September. Net groundwater exchange was calculated as the difference in discharge between upstream and downstream locations after correcting for channelized losses and gains (Eq 1), recognizing that evapotranspiration is unaccounted for using this approach:

$$Q_{gw} = (Q_{down} + Q_{out}) - (Q_{up} + Q_{in}) \quad (1)$$

where Q_{gw} is net groundwater exchange ($L \text{ sec}^{-1}$); Q_{down} is discharge at the downstream extent of the reach; Q_{out} is withdrawal via irrigation ditches; Q_{up} is discharge at the upstream extent of the reach; Q_{in} is inputs from channelized tributaries. With this approach, positive Q_{gw} values represent net groundwater discharge to the channel. The product of Q and concentration of any nutrient, x (C_x ; mg L^{-1}), yields material load (L), reported as kg d^{-1} . Mass-balance of nutrient loads over a given reach was calculated as the difference between outputs and inputs (Burns 1998):

$$\Delta L = (L_{down} + L_{out}) - (L_{up} + L_{in}) \quad (2)$$

where ΔL represents the net change in load (kg d^{-1}), positive values indicate load accumulation, and negative values indicate load decline.

Different characteristic concentrations were employed to determine nutrient loads contributing to or received from groundwater depending upon the direction of exchange. If Q_{gw} was negative (denoting groundwater recharge), we applied reach-specific daily mean surface water concentration to calculate change in load due to groundwater exchange (ΔL_{gw}); if Q_{gw} was positive (denoting groundwater discharge), we used the grand mean of groundwater concentration derived from the 19 wells. We then differentiated the putative roles of hydrology and biology on changes in nutrient loads using:

$$\Delta L_{bio} = \Delta L - \Delta L_{gw} \quad (3)$$

where the change in load due to biological processing (ΔL_{bio}) is equal to the difference between total change in load (ΔL) and the estimated change due to groundwater exchange (ΔL_{gw}). Hence, residual changes in load were attributed to biological processes. Negative ΔL_{bio} represents nutrient removal from the surface water (i.e., uptake), while positive ΔL_{bio} suggests addition to surface water via nutrient release (i.e., production). ΔL_{bio} for all nutrients was used to calculate areal processing rates (James et al. 2008), where

$$U = \frac{\Delta L_{bio}}{A} \quad (4)$$

U is areal processing ($\text{mg m}^{-2} \text{d}^{-1}$) and A is estimated whole-reach channel bed area (m^2). Positive U values represent nutrient release (i.e. production) and negative U values represent nutrient retention (i.e. uptake). We report both positive and negative U values to reflect losses (-) and gains (+) to surface water, respectively, and address potential mechanisms of solute processing among groundwater, benthic, and surface water compartments. Related spiraling metrics (sensu Newbold et al. 1981) are presented in the supplementary materials (Appendix G, H).

U_{NO_3} values > 0 were assumed to represent net nitrification rates because positive $\Delta L_{\text{bioNO}_3}$ is a net increase in NO_3^- load beyond hydrologic supply (i.e., via biologic production). Conversely, negative U_{NO_3} values are representative of net NO_3^- use without distinguishing between assimilatory or dissimilatory processes. Additionally, U_{DOC} values < 0 represent carbon (C) removal (i.e., net losses of DOC from the system).

2.5 Data Analysis

We used one-way ANOVA and Tukey's Honest Significant Difference (HSD) tests to distinguish physicochemical, hydrologic, morphologic, biologic, and biogeochemical characteristics among reaches. Normality and homogeneity of variance were assessed using the Shapiro-Wilk and Bartlett tests, respectively. Diagnostic plots were generated to visualize and assess normality and variance of residuals, and any potential outliers were identified with respect to Cook's distance. Non-normal data were log-transformed and parametric approaches employed when normality was achieved. Where appropriate, we used linear regression models to explore the effects of primary drivers on ecosystem function among reaches and seasons to identify potential controls on processing rates. For non-parametric assessments, we used the Kruskal-Wallis H and Mann-Whitney U tests to determine if reaches behaved differently. We used one-sample T-tests and the Wilcoxon signed rank test to determine if mean rates were significantly different from zero. All statistical assessments were performed in R (R Core Team 2013).

3.0 RESULTS

3.1 Aquatic Landscape Heterogeneity

Landscape morphologic attributes varied among reaches and generally transitioned from extensive flow-through wetlands to a single, entrenched stream channel with distance downstream (Figure 2, Appendix B). Whole-reach bed area decreased from $0.11 \pm 0.01 \text{ km}^2$ in

Reach I to $0.013 \pm 0.00093 \text{ km}^2$ in Reach IV (Figure 2, $P < 0.001$). Reach I included over 0.18 km^2 of open water, which was three times more than Reach II (0.046 km^2), and dwarfed Reaches III and IV (0.004 and 0.0028 km^2) as wetlands gave way to lotic channels (Figure 2). Similarly, floodplain wetland extent decreased from 2.34 km^2 in Reach I to 0.15 km^2 in Reach IV (Figure 2) and channel incision ratio increased from 0.49 in Reach I to 0.75 in Reach IV (Figure 2, $P < 0.001$).

Across the LCDC, reaches were distinguishable by physicochemical, hydrologic, biologic, and biogeochemical conditions (Table 1). In general, stream water was well oxygenated across all reaches (8.7 ± 0.8 to $10.9 \pm 1.2 \text{ mg L}^{-1}$ as mean \pm standard error) representing 99.4 ± 9.0 to $122.4 \pm 15.6 \%$ saturation (Table 1). Both mean temperature (12.2 ± 1.0 to $15.2 \pm 0.7 \text{ }^\circ\text{C}$) and specific electrical conductivity (349.5 ± 17.1 to $557.7 \pm 22.4 \text{ } \mu\text{S cm}^{-1}$) increased with distance downstream and differed among reaches ($P = 0.047$ and $P < 0.001$, respectively, Table 1). Water was alkaline with pH above 8.5 in all reaches (Table 1).

Hydrology also differed among reaches as wetlands gave way to stream channels. Median travel time was an order of magnitude greater in Reach I ($63.9 \pm 16.1 \text{ hr}$, $P < 0.001$) compared to Reaches II, III and IV (7.0 ± 1.1 , 4.8 ± 0.4 , $4.8 \pm 0.9 \text{ hr}$, respectively, Table 1). Average inflow to the reaches (Q_{up}) ranged from 664.6 ± 170.8 to $1,153.5 \pm 283.5 \text{ L s}^{-1}$ (Table 1). Channelized hydrologic gains and losses to the LCDC via tributary inputs or irrigation ditches were subject to atypical temporal variability due to their highly regulated nature. Flow was augmented by tributary inputs only in Reach I with an average inflow of $327.0 \pm 27.8 \text{ L s}^{-1}$ (Table 1). In contrast, only Reach IV was without irrigation withdrawal: channelized ditches removed from 208.7 ± 31.6 to $681.5 \pm 121.0 \text{ L s}^{-1}$ (Table 1). All reaches were subject to net groundwater discharge (Table 1), though of different magnitude among reaches ($P < 0.001$).

Mean Q_{gw} varied by more than 30-fold among reaches, but was only significantly different from zero in Reaches II and III. On average, Reach II gained $697.6 \pm 138.2 \text{ L s}^{-1}$ of groundwater, over twice that of Reach I and III (177.7 ± 107.6 and $239.0 \pm 87.1 \text{ L s}^{-1}$) and an order of magnitude greater than in Reach IV ($19.1 \pm 80.5 \text{ L s}^{-1}$, Table 1, Figure 3a). Net groundwater exchange in Reach II was distinct from the remaining reaches, as evidenced by the continuously positive Q_{gw} often two-fold greater than total surface water inputs (Figure 3b).

Throughout the study period, mean nutrient concentrations were relatively similar across the four reaches due to high temporal variability. Nitrate ranged from 0.12 ± 0.04 to $0.21 \pm 0.03 \text{ mg N L}^{-1}$ and was highest in Reaches II and III ($P = 0.084$). Ammonium was relatively low and stable, ranging from 0.01 ± 0.002 to $0.02 \pm 0.003 \text{ mg N L}^{-1}$ ($P = 0.51$). SRP concentrations were also relatively low and stable, and ranged from 0.02 ± 0.003 to $0.02 \pm 0.006 \text{ mg L}^{-1}$ ($P = 0.99$). Concentrations of DOC tended to increase downstream (2.36 ± 0.33 to $3.71 \pm 0.76 \text{ mg L}^{-1}$, Table 1), but differences were not significant ($P = 0.49$, Table 1).

Mean benthic chl-a was greatest in Reach I ($637.4 \pm 342.3 \text{ mg m}^{-2}$; $P < 0.05$) and tended to decline with distance downstream to Reach IV ($219.6 \pm 77.6 \text{ mg m}^{-2}$, Table 1). In contrast, BOM stocks were greater in Reach III ($305.4 \pm 72.0 \text{ g m}^{-2}$) and Reach I ($259.2 \pm 122.8 \text{ g m}^{-2}$) and lower in Reaches II and IV (183.2 ± 50.6 and $190.4 \pm 61.6 \text{ g m}^{-2}$, respectively, $P < 0.001$, Table 1). Mean percent organic matter of benthic samples ranged from $23.5 \pm 2.6\%$ in Reach I to $48.5 \pm 13.7\%$ in Reach II and values differed significantly among reaches ($P < 0.05$, Table 1). Mean autotrophic index ranged from 1.1 ± 0.2 to $2.3 \pm 0.8 \text{ mg chl-a:g AFDM}$ (Table 1).

3.3 Spatiotemporal Patterns in Biogeochemistry

Distinct biogeochemical signals were observed among reaches and over time. Synoptic sampling under contrasting flow regimes showed NO_3^- concentrations increased throughout

Reaches I and II, followed by a steady decline throughout Reaches III and IV (Figure 4a). During peak discharge in June, NO_3^- concentration increased from 0.032 ± 0.001 to 0.249 ± 0.006 mg N L^{-1} from Reach I to Reach II (Figure 4a), a 778% increase. Similarly, in August, NO_3^- concentration increased 688% along the same longitudinal extent, from 0.080 ± 0.011 to 0.551 ± 0.003 mg N L^{-1} . Higher concentrations in Reaches I and II were followed by steady declines in Reaches III and IV, especially in August (Figure 4a), a pattern also observed throughout the nine fixed sampling events (Appendix C). In contrast to striking changes in NO_3^- , NH_4^+ concentrations did not exhibit substantial spatial or temporal variation (Figure 4b) and remained low throughout the study period (0.017 ± 0.003 mg N L^{-1} , grand mean \pm standard error).

Concentrations of SRP and DOC in surface waters of the LCDC exhibited patterns that were unlike those observed for NO_3^- . Mean SRP concentrations were low and stable across all reaches and seasons (0.020 ± 0.003 mg L^{-1}) and did not exhibit substantial spatial or temporal variation (Figure 4c, Appendix C). In contrast to NO_3^- , DOC concentrations were greater during peak discharge (Figure 4d) and decreased during recession of the hydrograph (Appendix C). During peak runoff, DOC approached 9 mg L^{-1} in Reach III and IV before declining throughout the growing season to ca. 2 mg L^{-1} (Appendix C). While DOC concentration remained more or less unchanged across Reaches I and II during both synoptic samplings, it increased steadily through Reaches III and IV, from 3.97 ± 0.001 mg L^{-1} to 5.47 ± 0.001 mg L^{-1} in June ($P < 0.001$) and from 1.61 ± 0.007 to 3.63 ± 0.006 mg L^{-1} in August ($P < 0.001$, Figure 4d).

Tributary inputs to Reach I from Dutchman Creek (the only channelized inputs to any reach) had the highest mean (0.31 ± 0.018 mg N L^{-1}), maximum (0.52 ± 0.0091 mg N L^{-1}), and minimum (0.18 ± 0.0057 mg N L^{-1}) DIN concentrations of all 10 fixed sampling sites over the study period. Dutchman Creek SRP (0.019 ± 0.0014 mg L^{-1}) and DOC (2.42 ± 0.049 mg L^{-1})

concentrations were similar in magnitude to those of the four main stem reaches (Appendix D). Nutrient concentrations of irrigation withdrawals were dependent on position within the LCDC, reflecting surface water concentrations of the nearest main channel sampling site (Appendix D, E).

Groundwater nutrient concentrations did not exhibit clear spatial patterns across the wetland-stream sequence, but nutrient composition was distinct from corresponding surface water compartments for all constituents ($P < 0.001$, Figure 5). Mean groundwater NO_3^- concentration was strikingly low ($0.012 \pm 0.002 \text{ mg N L}^{-1}$) compared to the NO_3^- abundance in surface water (Figure 5). Ammonium and DOC averaged $0.18 \pm 0.029 \text{ mg N L}^{-1}$ and $18.83 \pm 4.45 \text{ mg L}^{-1}$, respectively, both substantially elevated in concentration compared to surface water (Figure 5). SRP concentration in groundwater averaged $0.033 \pm 0.006 \text{ mg L}^{-1}$, compared to $0.016 \pm 0.001 \text{ mg L}^{-1}$ in surfacewater (Figure 5). Across all reaches and seasons, there was a fourteen-fold increase in NO_3^- , a twelve-fold decrease in NH_4^+ , and a six-fold decrease in DOC concentration between groundwater and surface water compartments.

3.4 Nutrient Loads at Main Channel Sites

As the montane source water flowed through 23 km of the LCDC wetland-stream sequence, biogeochemical and hydrologic conditions changed substantially from MC1 to MC5. We found that stream discharge increased along the sequence by an average of 32%, whereas L_{NO_3} increased by 461%. Ammonium, SRP, and DOC loads exhibited similar changes over this longitudinal extent, increasing by 125, 132, and 133%, respectively (data not shown).

Nutrient loads at main channel sites varied by an order of magnitude across both space and time (Figure 6). Both NO_3^- and NH_4^+ loads followed U-shaped profiles from spring through the summer and into fall (Figure 6). Nitrate delivery was greatest in late spring and again during

fall at all main channel sites, approaching 30 kg N d^{-1} . A marked decline in L_{NO_3} occurred as the summer progressed, especially at sites downstream of irrigation withdrawals. During the summer period of reduced N delivery, surface water loads at MC1 and MC2 were 0.90 and 3.97 kg N d^{-1} , respectively, while MC3 exhibited the largest nitrate load (9.86 kg N d^{-1}). In contrast, L_{NO_3} at MC4 and MC5 were only 0.21 and 0.02 kg N d^{-1} , respectively. Autumnal increases in L_{NO_3} occurred at all sites and approached spring background conditions.

Material loads of NH_4^+ , SRP, and DOC also exhibited clear spatial and temporal patterns. L_{NH_4} patterns behaved similarly to L_{NO_3} during spring runoff, but were an order of magnitude lower, surpassing 3 kg N d^{-1} only at peak discharge (Figure 6). During the summer, mean L_{NH_4} was reduced to $< 1 \text{ kg N d}^{-1}$ at all main-channel sites (Figure 6). While L_{NH_4} rebounded slightly during late summer, delivery rates were not as high as observed during spring runoff. L_{SRP} and L_{DOC} spiked briefly at MC4 and MC5 in association with peak runoff, delivering over 10 and $2,000 \text{ kg d}^{-1}$, respectively, before declining steadily as the summer progressed (Figure 6). Compared to spring runoff, summertime loads were over an order of magnitude lower at all main-channel sites, delivering an average of $0.33 \pm 0.059 \text{ kg d}^{-1}$ and $88.52 \pm 22.35 \text{ kg DOC d}^{-1}$ and continued to decline throughout the study period (Figure 6).

3.5 Partitioning ΔL by Hydrology and Biology

Dissolved Inorganic N

Accumulation of nitrate was observed in all reaches on multiple sampling dates and differed significantly among reaches ($P < 0.05$). Mean ΔL_{NO_3} was positive and different from zero ($P < 0.05$) in Reaches I and II (6.08 ± 2.57 and $11.90 \pm 3.72 \text{ kg N d}^{-1}$, respectively, Figure 7, Appendix F). In contrast, total change in nitrate load was not different from zero ($P > 0.05$) in Reaches III ($0.75 \pm 3.93 \text{ kg N d}^{-1}$) and IV ($-0.56 \pm 1.31 \text{ kg N d}^{-1}$, Figure 7, Appendix F). On

average, ΔL_{gwNO_3} across all reaches was relatively small (-0.39 ± 0.51 to 0.73 ± 0.15 kg N d⁻¹), was different from zero only in Reach III ($P < 0.05$, Figure 7b), and represented a relatively small proportion (6-34%) of total change in load (Figure 7).

Average ΔL_{NH_4} was an order of magnitude lower than ΔL_{NO_3} , was significantly different from zero ($P < 0.05$) in all reaches except Reach IV, and did not differ significantly among reaches (Figure 7; $P = 0.24$). Mean ΔL_{NH_4} for Reaches I-IV was 0.22 ± 0.14 , 0.64 ± 0.27 , 0.81 ± 0.24 , and 0.25 ± 0.10 kg N d⁻¹, respectively. Potential NH_4^+ inputs from groundwater (i.e., ΔL_{gwNH_4}) were four to sixteen times greater than ΔL_{NH_4} (Figure 7). For instance, Reaches I and III received an average of 3.80 ± 1.19 and 3.90 ± 0.81 kg $\text{NH}_4\text{-N}$ d⁻¹ from groundwater, inputs an order of magnitude greater than ΔL_{NH_4} that evidently failed to manifest in altered surface water load (Figure 7, Appendix F). Moreover, Reach II received over 11.067 ± 0.64 kg $\text{NH}_4\text{-N}$ d⁻¹ from groundwater exchange, alongside negligible changes in total ΔL_{NH_4} . Reach IV received groundwater NH_4^+ inputs (1.44 ± 0.64 kg N d⁻¹) that were, on average, nearly six times ΔL_{NH_4} (0.25 ± 0.10 kg N d⁻¹, Figure 7, Appendix F).

Over time, Reach I and II were consistent and significant ($P < 0.05$) nitrate producers ($\Delta L_{\text{bioNO}_3}$; 6.46 ± 2.49 and 11.17 ± 3.71 kg N d⁻¹, respectively, Figure 7). In contrast, variability within Reaches III (0.64 ± 3.85 kg N d⁻¹) and IV (-0.37 ± 1.36 kg N d⁻¹) resulted in mean $\Delta L_{\text{bioNO}_3}$ not different from zero ($P > 0.05$, Figure 7). Mean $\Delta L_{\text{bioNH}_4}$ was negative for all reaches and different from zero in Reaches I, II, and III ($P < 0.05$), illustrating consistent NH_4^+ removal (Figure 7). Reaches I, III and IV demonstrated similar removal rates (-3.58 ± 1.12 , -3.09 ± 1.22 , and -1.18 ± 0.61 kg $\text{NH}_4\text{-N}$ d⁻¹, respectively), whereas NH_4^+ removal was three-fold greater in

Reach II, averaging $-10.43 \pm 2.25 \text{ kg N d}^{-1}$ (Figure 7). Together, $\Delta L_{\text{bioNO}_3}$ and $\Delta L_{\text{bioNH}_4}$ illustrated significant changes in DIN in Reaches I and II.

SRP and DOC

Mean ΔL_{SRP} was low across the LCDC (Figure 8, Appendix G), ranging from -0.97 ± 1.41 to $2.17 \pm 1.82 \text{ kg d}^{-1}$ and only significantly different from zero in Reach I ($P < 0.01$). Similarly, mean ΔL_{gwSRP} was low across the four reaches, ranging from -0.02 ± 0.28 to $1.96 \pm 0.39 \text{ kg d}^{-1}$, differing from zero in Reaches II and III ($P < 0.05$). Mean ΔL_{bioSRP} ranged from $-1.15 \pm 0.61 \text{ kg d}^{-1}$ in Reach II to $0.35 \pm 0.23 \text{ kg d}^{-1}$ in Reach I, but was not significantly different from zero in any reach ($P > 0.05$, Figure 8, Appendix G).

Overall, mean ΔL_{DOC} was positive in all reaches (Figure 8, Appendix G), but not significantly different from zero ($P > 0.05$) due to substantially different behaviors during peak and base flow conditions (Figure 4). On average, Reach I and IV exhibited slight increases in DOC load (11.23 ± 22.42 and $30.75 \pm 32.90 \text{ kg d}^{-1}$), whereas mean ΔL_{DOC} was over 200 kg d^{-1} in Reach II and III (Figure 8, Appendix G). Positive ΔL_{DOC} observed for all reaches paled in magnitude compared to the very large and significant estimates for ΔL_{gwDOC} . For instance, potential change in load due to groundwater inflow in Reach II (ΔL_{gwDOC} ; $1,134.90 \pm 224.83 \text{ kg d}^{-1}$) was nearly five times greater than the observed total change in load (i.e., ΔL_{DOC} ; $227.48 \pm 198.97 \text{ kg d}^{-1}$, Figure 8, Appendix G). Mean ΔL_{gwDOC} in Reach I and III were over 300 kg d^{-1} . Values for ΔL_{gwDOC} were significantly greater than zero ($P < 0.05$) in all reaches except Reach IV ($P = 0.27$), where ΔL_{gwDOC} was $105.05 \pm 87.85 \text{ kg d}^{-1}$ (Figure 8, Appendix G).

Given total changes in DOC load that were not different from zero and very strong positive changes associated with groundwater inputs, mean ΔL_{bioDOC} was negative in all reaches,

suggesting losses of DOC between ground- and surface water compartments. Despite seasonal variations, Reaches I and II exhibited average DOC removal rates of -364.66 ± 118.95 and $-907.42 \pm 294.28 \text{ kg d}^{-1}$, respectively, with both values significantly different from zero ($P = 0.016$ and 0.015). DOC removal rates in Reaches III ($-198.44 \pm 260.39 \text{ kg d}^{-1}$) and IV ($-74.31 \pm 60.54 \text{ kg d}^{-1}$) were also negative, but not significantly different from zero ($P > 0.05$, Figure 8, Appendix G). These data highlight the large differences between DOC concentration in ground- and surface water compartments and suggest retention or rapid consumption of DOC in the near-stream hyporheic zone, such that only a small proportion of the potential load enters the stream channel.

Biogeochemical Processing of Groundwater Nutrient Loads

The mass-balance for individual solute loads suggests active biogeochemical cycling at the stream-groundwater interface. In particular, all reaches exhibited negative $\Delta L_{\text{bioNH}_4}$ rates of the same order of magnitude as positive $\Delta L_{\text{bioNO}_3}$, suggesting relatively efficient biotic transformation of NH_4^+ to NO_3^- . Indeed, we found a significant relationship between ΔL_{NO_3} and ΔL_{gw} when treating groundwater as a single DIN pool ($r^2 = 0.17$, $P = 0.011$, Figure 9). Exclusion of a single outlier from Reach II enhanced explanatory power and resulted in a linear relationship with a slope near 1 (regression coefficient (β) = 1.1, $r^2 = 0.30$, $P < 0.001$, Figure 9) that predicts total change in NO_3^- load based on the magnitude of groundwater DIN exchange.

In contrast, we did not find strong evidence for groundwater as a driver of surface water DOC dynamics (Figure 9). Over all dates and reaches, ΔL_{gwDOC} was weakly related to ΔL_{DOC} ($r^2 = 0.10$, $P = 0.064$), the overall slope suggesting that only 30% of potential groundwater DOC inputs manifested as increases in surface water loads. Similarly, little evidence was found for linkages between ΔL_{gw} and ΔL for NH_4^+ ($r^2 = 0.062$; $P = 0.14$) or SRP ($r^2 = 0.026$; $P = 0.35$), and

low coefficients of determination suggest differing efficiencies of processing in the face of spatiotemporal variation (data not shown).

These data indicate the nutrient concentrations and loads were altered differently among the four designated reaches (Fig 7, 8, 10). Overall, materials entered the LCDC through MC1, exited the system at the downstream extent of Reach IV (MC 5), and exhibited spatial patterns that were relatively consistent over the study period regardless of irrigation withdrawals. Nitrate loads increased through Reaches I and II before declining slightly through Reaches III and IV (Figure 6). Ammonium and SRP loads typically increased with distance downstream, but did not show substantial accumulation (Figure 6). In contrast, DOC load increased with distance downstream particularly during the spring runoff period, but exhibited relatively low and stable loads across the LCDC through the summer months (Figure 6).

3.6 Rapid Nutrient Processing

Areal fluxes (U) for solute consumption ($-\Delta L_{\text{bio}}$) or production ($+\Delta L_{\text{bio}}$) provide ecosystem transformation rates that can be compared among reaches of the LCDC and with other aquatic ecosystems. Mean U_{NO_3} was positive and significantly different from zero ($P < 0.05$) for Reaches I and II (52.07 ± 19.84 , 257.63 ± 101.44 $\text{mg N m}^{-2} \text{d}^{-1}$) and not different from zero for Reach III (10.25 ± 139.96 $\text{mg N m}^{-2} \text{d}^{-1}$) and IV (-8.78 ± 101.71 $\text{mg N m}^{-2} \text{d}^{-1}$, Figure 10). Reaches I and II were also characterized by significant ($P < 0.05$) rates of C processing but, in contrast to acting as zones of NO_3^- production, they acted as net sinks for DOC loads. U_{DOC} was -2.93 ± 0.96 and -19.58 ± 5.82 $\text{g C m}^{-2} \text{d}^{-1}$, respectively, in the upstream reaches, and -8.29 ± 8.07 and -4.70 ± 4.00 $\text{g C m}^{-2} \text{d}^{-1}$ in Reaches III and IV where mean areal fluxes were not significantly different from zero ($P > 0.05$, Figure 10).

Ammonium and SRP exhibited contrasting processing dynamics. Mean U_{NH_4} was negative and significantly different from zero ($P < 0.05$) for Reach I, II, and III (-28.80 ± 8.98 , -226.25 ± 42.88 , $-123.54 \pm 43.34 \text{ mg N m}^{-2} \text{ d}^{-1}$, respectively) but not Reach IV ($-73.75 \pm 39.39 \text{ mg N m}^{-2} \text{ d}^{-1}$, Appendix H). U_{SRP} ranged from $-97.13 \pm 127.09 \text{ mg m}^{-2} \text{ d}^{-1}$ in Reach II to $45.05 \pm 55.92 \text{ mg m}^{-2} \text{ d}^{-1}$ in Reach I, but was not significantly different from zero ($P > 0.05$) for any of the four reaches (Appendix H).

Throughout the study period, Reaches I and II exhibited net nitrification (i.e., $U_{\text{NO}_3} > 0$) on all but one sampling date, versus 44 and 22% of dates in Reaches III and IV, respectively (Figure 10). Across the LCDC, individual measurements of net nitrification rates ranged from 9.07 to 807.72 $\text{mg N m}^{-2} \text{ d}^{-1}$, and the grand mean of U_{NO_3} values > 0 was 248.49 $\text{mg N m}^{-2} \text{ d}^{-1}$. Mean nitrification rates varied by reach, from $59.33 \pm 20.94 \text{ mg N m}^{-2} \text{ d}^{-1}$ in Reach I ($n = 8$) to $493.58 \pm 136.40 \text{ mg N m}^{-2} \text{ d}^{-1}$ in Reach IV ($n = 2$). While Reach III exhibited the single highest rate, Reach II exhibited more consistent nitrification, averaging $323.05 \pm 64.87 \text{ mg N m}^{-2} \text{ d}^{-1}$ over eight sampling dates with $U_{\text{NO}_3} > 0$ (data not shown).

Across all reaches and throughout the study period, net C loss ($U_{\text{DOC}} < 0$) varied by three orders of magnitude and occurred on 75% of sample events (Figure 10). C loss rates ranged from -0.059 to $-54.91 \text{ g C m}^{-2} \text{ d}^{-1}$, and averaged $-14.60 \pm 2.73 \text{ g C m}^{-2} \text{ d}^{-1}$. Reach II had the highest mean loss rate ($-23.24 \pm 5.14 \text{ g C m}^{-2} \text{ d}^{-1}$), followed by Reach III (-16.74 ± 6.80), IV (-12.78 ± 4.069), and I ($-3.87 \pm 0.95 \text{ g C m}^{-2} \text{ d}^{-1}$, data not shown).

4.0 DISCUSSION

Evidence shows that heterogeneous hydrologic (Zarnetske et al. 2011, Lottig et al. 2013), geomorphic (Gücker and Boëchat. 2004, Helton et al. 2011), and biologic conditions (Ribot et al.

2012) across aquatic landscapes may result in stream reaches with differing nutrient concentrations (Arango et al. 2007), processing capacities (Ensign and Doyle 2006), and material fates (Tobias et al. 2001). This has been attributed to the capacity for these factors to influence biotic uptake, storage, production, and removal. We used biogeochemical loads, a useful measurement of nutrient production, transformation, and conveyance (James 2009), to show how linked aquatic ecosystems interact to generate emergent signals at the landscape scale. We observed strong spatial and temporal variability in the form, concentration, and processing rates of DIN and DOC throughout the LCDC. Overall, the wetland-stream sequence exhibited robust signals of NO_3^- production concomitant with NH_4^+ and DOC removal. Moreover, the distribution of distinct biogeochemical signals along the sequence indicates the existence of discrete NPDs and a spatial gradient in the tendency for a given NPD to shift in character. Observed shifts in NPD character reflect variability in hydrologic linkages between subsurface and surface resource pools. In particular, we found substantial loads of DIN entering the stream channel via wetland or groundwater flow paths, and their ultimate fate and form resulted from a combination of local and routing controls that drove NPD behavior.

4.1 Hydro-geomorphic Controls in the LCDC

Much of the variability in biogeochemical conditions along the LCDC sequence can be elucidated by the distinct structure of the four study reaches. Profiles of hydro-geomorphic structure illustrate the decrease in wetland extent, whole-reach bed area, residence time, and open water from Reach I to Reach IV. This reflects a transition from systems dominated by flow-through wetlands to those progressively more lotic in character. Reaches I, II, and III often received substantial groundwater inputs and typically behaved as gaining reaches, whereas Reach IV demonstrated minimal groundwater discharge. Along this transitional sequence, variable hydrologic gains and losses influence nutrient dynamics and groundwater exchange acts

as a primary driver of N loads. Our data suggest these hydro-geomorphic interactions shape the system, prompting distinct biological responses that result in characteristic biogeochemical behaviors.

Nitrogen Dynamics

Flow entering the LCDC is derived from a montane canyon that provides cold, low-N water. In Reaches I and II, this source water accumulates NO_3^- along flow paths transcending a peat fen, a lentic water body, and extensive flow-through wetlands. In Reaches III and IV, NO_3^- concentration declines as the landscape transitions from hydrologically-connected wetlands to more incised, lotic channels. Strongly positive ΔL_{NO_3} values in Reaches I and II reflect an accumulation (production) of NO_3^- greater in magnitude than provided by groundwater NO_3^- inputs alone. The resulting $\Delta L_{\text{bioNO}_3}$ and U_{NO_3} rates (values > 0) suggest nitrification of incoming groundwater NH_4^+ . Conversely, the negative U_{NO_3} values (removal) measured on individual sampling events in Reaches III and IV, and the negative mean U_{NH_4} values in Reaches I-III, reflect N removal dynamics that are more typical of low-order stream ecosystems (Peterson et al. 2001, Mulholland et al. 2008). Our range of negative U values from the LCDC are similar to the median fluxes reported across numerous stream systems in both the LINX I ($U_{\text{NO}_3} = -42.0$ and $U_{\text{NH}_4} = -62.1 \text{ mg N m}^{-2} \text{ d}^{-1}$, Webster et al. 2003) and LINX II ($U_{\text{NO}_3} = -53.55$ and $U_{\text{NH}_4} = -38.07 \pm 160.10 \text{ mg N m}^{-2} \text{ d}^{-1}$, Mulholland et al. 2008) studies of N dynamics in lotic systems (published rates converted to negative values to reflect N removal as reported in this study).

Groundwater NH_4^+ inputs to Reaches I and II account for much of the observed increase in NO_3^- load (assuming nitrification was the dominant process), and this NH_4^+ may be provided, in part, by ammonification of wetland organic matter that enters the stream. Buildup of organic N in wetlands and subsequent mineralization produces solutes that can elevate stream water

concentrations (Lottig et al. 2013). Across 119 watersheds, Pellerin et al. (2004) found that wetland extent alone predicted up to 60% of the variability in dissolved organic N (DON) concentration in drainage waters. In the LCDC, both Reaches I and II are rich in benthic autotrophic biomass and organic matter, and the adjacent wetlands reflect those typical of floodplain systems that accumulate both sediment and dead plant matter (U.S. EPA and CDM Smith 2012). Along surface and groundwater flow paths, DON is subject to ammonification and results in NH_4^+ production, which can ultimately oxidize to NO_3^- via nitrification (Starry et al. 2005). The decomposition of wetland organic matter and subsequent increase in stream DIN through Reaches I and II could be one mechanism that explains both elevated NH_4^+ concentrations in groundwater and longitudinal increases in stream NO_3^- load.

Wetland organic matter mineralization and subsequent delivery of inorganic solutes to streams are strongly influenced by flow path dynamics and chemical conditions. Jones and Holmes (1996) found the hydrology of fluvial wetlands and hyporheic zones exhibit strong control over N transformations and export to streams depending on flow path length and substrate form (i.e., NH_4^+ vs. NO_3^-). This is because organic N is reduced and oxidized under contrasting conditions that often reflect the predominance of stream or wetland settings. Wolf et al. (2013) found that floodplain wetlands exhibit high ammonification rates and, depending on hydrologic conditions, can provide substantial N delivery to downstream systems. In a study comparing linked flow-through wetlands and stream reaches, Powers et al. (2012) found that wetlands were less efficient at NO_3^- removal per unit area than their stream counterparts. Moreover, Sponseller et al. (2018) reported that headwater peat mires act as disproportionately high NH_4^+ sources to downstream surface waters. This was shown to be a result of groundwater transport of wetland-derived NH_4^+ through deep catotelm (biologically inactive peat layers) flow

paths which bypass the active, shallow soil layers. Such studies demonstrate how the reducing conditions typically associated with organic matter-rich wetlands have the potential to release NH_4^+ , whereas stream conditions favor the oxidization/consumption of NH_4^+ and retention of NO_3^- . Although we did not measure N processing at sub-ecosystem scales (i.e., individual flow-through wetlands), the greatest net NO_3^- production occurred in wetland-dominated reaches. This is in contrast to the fluvial wetlands and surface transient storage zones that behaved as net removers of NO_3^- as reported by Wollheim et al. (2014). However, our results agree with the suggestion by Wollheim et al. (2014) that flow-through wetlands can act as biogeochemical hot spots with elevated N reaction rates compared to streams alone. Our results further suggest that N form, as well as local and routing controls (i.e. redox conditions and direction of groundwater exchange) ultimately dictate the primary processes and biogeochemical signals at the landscape scale. Together, these findings show how groundwater and wetland flow paths may route reduced N to the stream channel in the LCDC, where it is converted to NO_3^- . These linked biogeochemical mechanisms, driven in part by geomorphic structure and hydrologic connectivity, suggest that the drastic increase in surface water NO_3^- observed in Reaches I and II is a result of nitrification of reduced N.

Net nitrification rates in the LCDC (derived from positive U_{NO_3} values) span a broad range of rates reported in the literature for streams and indicate significant transformation of N loads in this wetland-stream. Rates of lower magnitude in the LCDC are similar to those found in studies of low-order streams by Hamilton et al. (2001), Dodds et al. (2000), and Strauss and Lamberti (2002) (Figure 11). Grimm et al. (1991) reported nitrification rates up to $64.5 \text{ mg N m}^{-2} \text{ d}^{-1}$ in a Sonoran Desert stream, a rate comparable to the mean in Reach I of the LCDC ($59.33 \text{ mg N m}^{-2} \text{ d}^{-1}$). The upper end of our reported range, however, reflects rates an order of magnitude

greater than observed for most stream and natural wetland ecosystems (Andersen and Hansen 1982, Bowden 1986, Zak and Grigal 1991). Furthermore, these rates are elevated in comparison to those measured in lake sediments (Bruesewitz et al. 2012) or backwaters of the Mississippi, where James (2009) found that anoxic conditions inhibited nitrification in an NH_4^+ -rich setting (Figure 11). Reach II demonstrated prolific nitrification, with average rates of similar magnitude to those measured in oxygenated surface-flow constructed treatment wetlands (SFCTW) receiving sewage effluent (Palmer et al. 2009, Figure 11).

The reported variation in nitrification rates among these disparate systems might be explained by substrate (NH_4^+) availability. For instance, the LCDC has a substantial NH_4^+ source from groundwater inputs, whereas the streams mentioned above had markedly lower DIN concentrations. Peterson et al. (2001) reported nitrification rates over $80 \text{ mg N m}^{-2} \text{ d}^{-1}$ in low- NH_4^+ ($< 0.01 \text{ mg L}^{-1}$) streams, where 70-80% of NH_4^+ was removed by the stream bottom. Our system demonstrated 92% NH_4^+ transformation when considering the grand means of ground- and surface water concentrations, resulting in minimal NH_4^+ in stream water. In settings where NH_4^+ is not limiting and oxygen is plentiful, nitrification rates can exceed those typically reported. Kemp and Dodds (2002) demonstrated $> 300\%$ increases in nitrification rates with maximum rates of $35 \text{ mg N m}^{-2} \text{ d}^{-1}$ in streams following NH_4^+ amendments of up to 0.025 mg L^{-1} . These conditions likely exist in the hyporheic zone of the LCDC, where oxygen-saturated surface water interfaces with anoxic interstitial groundwater, optimizing nitrification potential (Zarnetske et al. 2012). In gaining reaches of the LCDC, it is likely that oxygen-depleted, NH_4^+ -rich groundwater enters the stream through the hyporheic zone where it is exposed to aerobic conditions and extensive microbial communities. Indeed, the interface of surface and shallow groundwater has been shown to greatly influence N (Jones and Holmes 1996) and DOC (Findlay

et al. 1993) concentrations, in part due to large gradients in redox conditions that lead to coupled processes such as nitrification-denitrification and precipitation-adsorption (Marzadri et al. 2012; Sudoh et al. 2015). The lowest of our estimated net nitrification rates agree with those reported in studies characterized by streams with low NH_4^+ concentrations (i.e., those similar or lower than values observed in LCDC surface waters). Conversely, our maximum rates approached those of sewage-augmented treatment wetlands (Fig. 11), suggesting that certain reaches of the LCDC obtained much higher nitrification rates because of enhanced NH_4^+ supply. High nitrification rates in the LCDC support river network studies that suggest a substantial portion of N loads can be transformed within linked stream ecosystems (Koenig et al. 2017), and provide evidence of the ‘shunting’ of NO_3^- to downstream reaches (Raymond et al. 2016).

This study highlights the influence of groundwater exchange and flow-through wetlands on reach scale N dynamics, demonstrates the existence of discrete NPDs along a wetland-stream sequence, and illustrates the spatiotemporal variation in nutrient loads, processing capacities, and material fates as they relate to hydrologic, geomorphic, and biologic conditions. The flow-through wetlands positioned along the LCDC sequence may influence NPD character as distinct hydro-geomorphic conditions promote surface-groundwater interaction, enhance mineralization of organic matter, and enable export of NH_4^+ to the stream, where conditions support high nitrification and N processing rates. When considering nutrient processes as domains in functional space, we see a shift in character with distance downstream: from N production in Reaches I and II, to mixed production-consumption in Reach III, to an increasing tendency towards net consumption in Reach IV. The lower two reaches of the LCDC behave more similar to low-order streams in the literature due to the diminishing role of flow-through wetlands and a ‘shunted’ NO_3^- source from which in-stream processes can draw. While Reach I and II act as

NO_3^- producers due to groundwater and wetland influences, Reach III and IV exhibit process dynamics that suggest a progressive transition to NO_3^- consumption with increasing distance downstream.

Carbon Dynamics

Wetland-dominated stream reaches are often characterized by elevated DOC concentrations (Lottig et al. 2013) due to mineralization of organic matter stored in wetland soils and transport of solutes to streams. However, longitudinal patterns of DOC concentration in the LCDC were not congruent with the extent of wetland area proximate to a given reach. The most wetland-dominated reaches (I and II) did not exhibit elevated DOC concentrations in comparison to the reaches characterized by lotic channels with substantially lower wetland extent but slightly higher DOC levels. Moreover, ΔL_{DOC} values remained relatively unchanged across all reaches of the wetland-stream sequence, suggesting that adjacent flow-through wetlands had relatively little influence on DOC dynamics in the surface waters of the LCDC. Coupling groundwater discharge with DOC concentrations, on the other hand, resulted in ΔL_{bio} values, and thus U_{DOC} rates, that were strongly negative in Reach I and II. This reflects retention or removal of DOC in the hyporheic zone between groundwater and surface water compartments.

Any attempt to generalize DOC processing in stream ecosystems is fraught with compounding factors related to DOC quality and composition (Strauss and Lamberti 2002, Stelzer et al. 2003). In streams, DOC represents a complex mixture of compounds that varies from highly reactive (i.e. glucose) to more recalcitrant forms that exhibit substantially different mineralization rates and present a critical challenge to understanding and modeling C processing (Mineau et al. 2016). Labile DOC additions have been shown to have a priming effect on C processing (Thouin et al. 2009) as well as inhibit nitrification as metabolically-stimulated

heterotrophic bacteria outcompete nitrifying bacteria for NH_4^+ (Strauss and Lamberti 2002). Furthermore, less labile ambient (stream water) DOC has been shown to sorb quite rapidly to hyporheic sediments (Findlay and Sobczak 1996). The variable biological and chemical reactivity of DOC compounds adds a level of uncertainty to C balances that attempt to differentiate between biological removal and physical or chemical retention. However, while we did not directly measure DOC quality or composition in the LCDC, mass-balance assessments illustrate the substantial capacity of wetland-streams to transform and retain C.

As it did for N species, C mass balance in the LCDC showed contrasting character and magnitude of C processing among reaches. Assuming C loss (i.e., $U_{\text{DOC}} < 0$) was due solely to respiratory consumption, our estimates were substantially greater than the highest ecosystem respiration values reported for net heterotrophic streams and rivers (Meyer and Edwards 1990, Lupon et al. 2016, Figure 11). For instance, Hall et al. (2016) estimated respiration to be $-5.78 \text{ g C m}^{-2} \text{ d}^{-1}$ in a rocky mountain stream in Idaho, while others have reported values between -0.20 (Hitchcock et al. 2010) and $-2.07 \text{ g C m}^{-2} \text{ d}^{-1}$ (Fisher et al. 1982). The mean C flux in Reach I ($-3.87 \text{ g C m}^{-2} \text{ d}^{-1}$) fell within the typically reported range, while the other three reaches of the LCDC exhibited C fluxes an order of magnitude greater than most streams. The C flux in Reaches II to IV of the LCDC were greater than ecosystem respiration estimates from 72 streams comparing land use across eight regions (Bernot et al. 2010), and greater still than measurements in C-rich settings such as estuaries (Caffrey et al. 2014, Hitchcock et al. 2010, Maher et al. 2013, Nidzieko et al. 2014), peatlands (McConnell et al. 2013), and wetlands (Maynard et al. 2012, Figure 11).

These uncharacteristically high C fluxes suggest pathways other than solely respiratory consumption as mechanisms for DOC removal. DOC adsorption may be of particular importance

in the LCDC given extant geochemical conditions. Field observations indicate the presence of substantial (> 1 cm) calcareous deposits along the LCDC waterways consistent with the alkaline pH reported for surface waters. Plentiful calcareous minerals in part reflect local geology (U.S. EPA & CDM Smith 2004, NRCS 2018), but may be related to reclamation activities in the LCDC uplands, where lime (CaCO_3) was applied at rates up to 8 tons per acre in 2008-2009 (MT NRDP 2007). Calcium carbonate precipitation at the surface-ground water interface may contribute to C loss as groundwater DOC adsorbs to surfaces of CaCO_3 particles. Indeed, Sudoh et al. (2015) demonstrated that DOC (humic acids) concentrations in river water consisting of 33.4 mg L^{-1} declined to 4.5 mg L^{-1} when treated with CaCO_3 , an 87% removal rate. Findlay and Sobczak (1996) found DOC adsorption to hyporheic sediments explained consistently high retention rates, even under conditions unsuited for biotic DOC uptake. Elevated percent organic matter values in LCDC benthic biomass slurries support the adsorption of DOC to precipitated carbonates on stream cobbles at the hyporheic zone-stream interface. While adsorption of DOC to carbonate particles is dependent on concentration, composition, and surface charge, findings from Bob and Walker (2001) suggest retention rates peak in alkaline conditions like those found in the LCDC. Our coarse estimations of DOC loss are substantially greater than published ecosystem respiration estimates and may reflect a combination of biological and chemical removal of DOC.

4.2 Effects of Management Practices on NPD Character

Land use (Groffman et al. 2004, Walter and Merritts 2008) and stream flow regulation (Poff et al. 2007) have clear impacts on watershed biogeochemical and hydrologic conditions because of how they influence the exogenous inputs of nutrients (Pennino et al. 2016) and disrupt natural flow and sediment regimes (Renwick et al. 2005). In the LCDC, these influences are evidenced by 1) the potential for the N source supporting the elevated nitrification rates to be

related to municipal wastewater management practices and 2) the large abstraction of channel water for agricultural use. The Dutchman Creek tributary flowing into Reach I consistently exhibited the highest DIN concentrations across the entire LCDC, and is located ca. 4 km downstream of the municipal infiltration basins (Figure 1). The infiltration basins and adjacent agricultural fields often receive wastewater applications as part of the treatment process and could act as an N source to the LCDC. While actual contributions remain unknown, it is possible that much of the N we observed entering the stream via groundwater and wetland flow paths is ultimately derived from this facility. In that case, exogenous N from anthropogenic activities could have significant impacts on the character and magnitude of NPDs as it pertains to substrate availability. The proportion of N in the LCDC derived from wetland mineralization or anthropogenic inputs warrants further investigation, as efforts could be taken to minimize N loads from municipal sources.

Irrigation withdrawals also substantially influenced the hydrology and biogeochemistry of the LCDC. During mid-summer, the vast majority of channel water is routinely diverted from Reach III to meet agricultural demands. During 2018, withdrawal of this type had profound impacts on the magnitude of nutrient loading rates as well as biological nutrient fluxes, such that areal processing rates for NO_3^- suddenly shifted from positive (producer) to negative (consumer), and then returned back to positive once the diversion was removed (Figure 10). During base flow in Reach III, ΔL_{gwNO_3} was low while ΔL_{gwNH_4} was an order of magnitude greater. Both remained relatively stable despite diversion, suggesting that groundwater N supply was not responsible for the shift in NPD dynamics. The great reduction in flow downstream of the diversion dam likely increased biologic processing and retention of N by stream channel biota (Martí et al. 1997, Zarnetske et al. 2011), resulting in the observed NPD shift from NO_3^- producer to consumer.

This event shows the capacity for dramatic shifts in NPD character in response to human alteration of hydrologic and material loading rates. It also demonstrates the plasticity of stream ecosystems and biogeochemical fates in response to anthropogenic influences on local and routing controls.

5.0 CONCLUSION

This study characterized a wetland-stream sequence to better understand landscape-scale hydro-geomorphic and biogeochemical processes across multiple linked aquatic ecosystems. The mass-balance approach yielded material loading rates and reflected ecosystem-level processes at large spatial and temporal scales. This study identified groundwater exchange as an important driver of DIN loads, processing rates, and fate in streams characterized by extensive flow-through wetlands. Estimates of DOC removal highlight additional C processes that may complement biological consumption. Our findings suggest that the position of stream reaches in relation to wetland hydro-geomorphology can dictate NPD behavior and influence nutrient source-sink dynamics. The ability to comprehend, quantify, and locate biogeochemical functions at broad spatial extents is critical for the informed management of fluvial ecosystems, particularly those transporting constituents of ecological concern. The methods employed and information gleaned from this study are readily transferable to other watersheds with nutrient management issues, particularly those subject to groundwater and agricultural abstraction influences. Applying a sensible landscape approach to stream and wetland nutrient dynamics is a critical step to better understand and manage low-order streams with potential watershed-scale influences.

6.0 LITERATURE CITED

- Andersen, F.O. and J. E. Hansen. 1982. Nitrogen cycling and microbial decomposition in sediments with *Phragmites australis* (*Poaceae*). *Hydrobiological Bulletin* 16(1): 11-19.
- APHA. 1999. Standard methods for the examination of water and wastewater: Method 4500Norg-C. American Public Health Association, Washington, D.C.
- Arango, C. P., J. L. Tank, J. L. Schaller, T. V. Royer, M. J. Bernot, and M. B. David. 2007. Benthic organic carbon influences denitrification in streams with high nitrate concentration. *Freshwater Biology* 52:1210–1222.
- Bernot, M. J., D. J. Sobota, R. O. Hall, P. J. Mulholland, W. K. Dodds, J. R. Webster, J. L. Tank, L. R. Ashkenas, L. W. Cooper, C. N. Dahm, S. V. Gregory, N. B. Grimm, S. K. Hamilton, S. L. Johnson, W. H. McDowell, J. L. Meyer, B. Peterson, G. C. Poole, H. M. Valett, C. Arango, J. L. Beaulieu, A. J. Burgin, C. Crenshaw, A. M. Helton, L. Johnson, J. Merriam, B. R. Niederlehner, J. M. O'Brien, J. D. Potter, R. W. Sheibley, S. M. Thomas, and K. Wilson. 2010. Inter-regional comparison of land-use effects on stream metabolism. *Freshwater Biology* 55:1874–1890.
- Bilby, R. E., and G. E. Likens. 1980. Importance of organic debris dams in the structure and function of stream ecosystems. *Ecology* 61:1107–1113.
- Bob, M., and H. W. Walker. 2001. Enhanced adsorption of natural organic matter on calcium carbonate particles through surface charge modification. *Colloids and Surfaces* 191:17–25.

- Bowden WB. 1986. Nitrification, nitrate reduction, and nitrogen immobilization in a tidal freshwater marsh sediment. *Ecology* 67(1): 88-99
- Brinson, M. M. 1993. Changes in the functioning of wetlands along environmental gradients. *Wetlands* 13:65–74.
- Brookshire, E. N. J., H. M. Valett, S.A. Thomas, and J. R. Webster. 2005. Coupled cycling of dissolved organic nitrogen and carbon in a forest stream. *Ecology* 86:2487–2496.
- Bruesewitz, D. A., J. L. Tank, and S. K. Hamilton. 2012. Incorporating spatial variation of nitrification and denitrification rates into whole-lake nitrogen dynamics. *Journal of Geophysical Research: Biogeosciences* 117:1–12.
- Burns, D. A. 1998. Uptake of NO₃ in an upland stream environment: A mass balance approach. *Biogeochemistry* 40:73–96.
- Caffrey, J. M., M. C. Murrell, K. S. Amacker, J. W. Harper, S. Phipps, and M. S. Woodrey. 2014. Seasonal and inter-annual patterns in primary production, respiration, and net ecosystem metabolism in three estuaries in the northeast Gulf of Mexico. *Estuaries and Coasts* 37:222–241.
- Caldwell, S. K., M. Peipoch, and H. M. Valett. 2015. Spatial drivers of ecosystem structure and function in a floodplain riverscape: springbrook nutrient dynamics. *Freshwater Science* 34:233–244.
- Coats, N., and R. Goldman. 2001. Patterns of nitrogen transport in streams of Lake Tahoe basin, California-Nevada. *Water Resources* 37:405–415.

- Dodds, W. K., M. A. Evans-White, N. M. Gerlanc, L. Gray, D. A. Gudder, M. J. Kemp, A. L. López, D. Stagliano, E. A. Strauss, J. L. Tank, M. R. Whiles, and W. M. Wollheim. 2000. Quantification of the nitrogen cycle in a prairie stream. *Ecosystems* 3:574–589.
- Doyle, M. W., E. H. Stanley, and J. M. Harbor. 2003. Hydro-geomorphic controls on phosphorus retention in streams. *Water Resources Research* 39:1–17.
- Elser, J. J., and B. L. Kimmel. 1985. Nutrient availability for phytoplankton production in a multiple-impoundment series. *Canadian Journal of Fisheries and Aquatic Sciences* 42:1359–1370.
- Ensign, S. H., and M. W. Doyle. 2006. Nutrient spiraling in streams and river networks. *Journal of Geophysical Research: Biogeosciences*. 111:1–13.
- Fellows, C. S., H. M. Valett, C. N. Dahm, P. J. Mulholland, and S. A. Thomas. 2006. Coupling nutrient uptake and energy flow in headwater streams. *Ecosystems* 9:788–804.
- Findlay, S. E. G., and W. V. Sobczak. 1996. Variability in removal of dissolved organic carbon in hyporheic sediments. *Journal of the North American Benthological Society* 15:35–41.
- Findlay, S. E. G., D. Strayer, C. Goumbala, and K. Gould. 1993. Metabolism of stream water dissolved organic carbon in the shallow hyporheic zone. *Limnology and Oceanography* 38:1493–1499.
- Fisher, S. G., J. Gray, N. B. Grimm, and D. E. Busch. 1982. Temporal succession in a desert stream ecosystem following flash flooding. *Ecological Monographs* 52:93–110.

- Fisher, S. G., R. A. Sponseller, and J. B. Heffernan. 2004. Horizons in stream biogeochemistry: Flow paths to progress. *Ecology* 85:2369–2379.
- Gordon, N., T. McMahon, and B. Finlayson 1992. *Stream hydrology: An introduction for ecologists*, John Wiley, New York.
- Gorham, E. 1991. Biogeochemistry: its origins and development. *Biogeochemistry* 13:199–239.
- Grimm, N. B., H. M. Valett, E. H. Stanley, and S. G. Fisher. 1991. Contribution of the hyporheic zone to stability of an arid-land stream: *Internationale Vereinigung fuer Theoretische und Angewandte Limnologie* 24(3): 1595 – 1599.
- Groffman, P. M., N. L. Law, K. T. Belt, L. E. Band, and G. T. Fisher. 2004. Nitrogen fluxes and retention in urban watershed ecosystems. *Ecosystems* 7:393–403.
- Gücker, B., and I. G. Boëchat. 2004. Stream morphology controls ammonium uptake in tropical headwaters. *Ecology* 85:2818–2827.
- Hall, R. O., J. L. Tank, M. A. Baker, E. J. Rosi-Marshall, and E. R. Hotchkiss. 2016. Metabolism, gas exchange, and carbon spiraling in rivers. *Ecosystems* 19:73–86.
- Hall, R. O., M. A. Baker, E. J. Rosi-Marshall, J. L. Tank, and J. D. Newbold. 2013. Solute-specific scaling of inorganic nitrogen and phosphorus uptake in streams. *Biogeosciences* 10:7323–7331.
- Hamilton, S. K., J. L. Tank, F. David, W. M. Wollheim, B. J. Peterson, and J. R. Webster. 2001. Nitrogen uptake and transformation in a Midwestern U.S. stream: A stable isotope enrichment study. *Biogeochemistry* 54:297–340.

- Helton, A. M., G. C. Poole, J. L. Meyer, W. M. Wollheim, B. J. Peterson, P. J. Mulholland, E. S. Bernhardt, J. A. Stanford, C. Arango, L. R. Ashkenas, L. W. Cooper, W. K. Dodds, S. V. Gregory, R. O. Hall, S. K. Hamilton, S. L. Johnson, W. H. McDowell, J. D. Potter, J. L. Tank, S. M. Thomas, H. M. Valett, J. R. Webster, and L. Zeglin. 2011. Thinking outside the channel: Modeling nitrogen cycling in networked river ecosystems. *Frontiers in Ecology and the Environment* 9:229–238.
- Hitchcock, G. L., G. Kirkpatrick, P. Minnett, and V. Palubok. 2010. Net community production and dark community respiration in a *Karenia brevis* (*Davis*) bloom in West Florida coastal waters, USA. *Harmful Algae* 9:351–358.
- Houser, J. N., P. J. Mulholland, and K. O. Maloney. 2005. Catchment disturbance and stream metabolism: Patterns in ecosystem respiration and gross primary production along a gradient of upland soil and vegetation disturbance. *Journal of the North American Benthological Society* 24:538–552.
- Ingman, G., M.A. Kerr. 1990. Nutrient sources in the Clark Fork River basin. Clark Fork Symposium Archives. Retrieved 5 May 2018 from <https://scholarworks.umt.edu/cgi/viewcontent.cgi?article=1208&context=clarkforksymposium>
- James, W. F., W. B. Richardson, and D. M. Soballe. 2008. Contribution of sediment fluxes and transformations to the summer nitrogen budget of an Upper Mississippi River backwater system. *Hydrobiologia* 598:95–107.
- James, W.F. 2009. Nitrogen retention in a floodplain backwater of the upper Mississippi River (USA). *Aquatic Sciences* 72:61–69.

- Jones, J. B., and R. M. Holmes. 1996. Surface-subsurface interactions in stream ecosystems. *Trends in Ecology and Evolution* 11(6):239–242.
- Junk, W. J., P. B. Bayley, and R. E. Sparks. 1989. The flood-pulse concept in river-floodplain systems. *Proceedings of the International Large River Symposium* (106).
- Kemp, M., and W. Dodds. 2002. The influence of ammonium, nitrate, and dissolved oxygen concentrations on uptake, nitrification, and denitrification in prairie stream substrata. *Limnology and Oceanography* 47:1380–1393.
- Kling, G. W., G. W. Kipphut, M. M. Miller, and J. O. O’Briens. 2000. Integration of lakes and streams in a landscape perspective: the importance of material processing on spatial patterns and temporal coherence. *Freshwater Biology* 43:477–497.
- Koenig, L. E., C. Song, W. M. Wollheim, J. Rüegg, and W. H. McDowell. 2017. Nitrification increases nitrogen export from a tropical river network. *Freshwater Science* 36:698–712.
- Kuglerova, L., R. Jansson, R. A. Sponseller, H. Laudon, and B. Malm-Renöfält. 2015. Local and regional processes determine plant species richness in a river-network metacommunity. *Ecology* 96:381–391.
- Lottig, N. R., I. Buffam, and E. H. Stanley. 2013. Comparisons of wetland and drainage lake influences on stream dissolved carbon concentrations and yields in a north temperate lake-rich region. *Aquatic Sciences* 75:619–630.

- Lupon, A., E. Martí, F. Sabater, and S. Bernal. 2016. Green light: gross primary production influences seasonal stream N export by controlling fine-scale N dynamics. *Ecology* 97:133–144.
- Maher, D. T., I. R. Santos, L. Golsby-Smith, J. Gleeson, and B. D. Eyre. 2013. Groundwater-derived dissolved organic carbon exports from a mangrove tidal creek: The missing mangrove carbon sink? *Limnology and Oceanography* 58(2): 475-488.
- Martí, E., N. B. Grimm, and S. G. Fisher. 1997. Pre- and post-flood uptake efficiency of nitrogen in a Sonoran Desert stream. *Journal of the North American Benthological Society* 16:805–819.
- Marzadri, A., D. Tonina, and A. Bellin. 2012. Morphodynamic controls on redox conditions and on nitrogen dynamics within the hyporheic zone: Application to gravel bed rivers with alternate-bar morphology. *Journal of Geophysical Research: Biogeosciences* 117:1–14.
- Meyer, J. L., and R. T. Edwards. 1990. Ecosystem metabolism and turnover of organic carbon along a blackwater river continuum. *Ecology* 71:668–677.
- Mineau, M. M., W. M. Wollheim, I. Buffam, S. E. G. Findlay, R. O. Hall, E. R. Hotchkiss, L. E. Koenig, W. H. McDowell, and T. B. Parr. 2016. Dissolved organic carbon uptake in streams: A review and assessment of reach-scale measurements. *Journal of Geophysical Research: Biogeosciences* 121:2019–2029.

- Montana Department of Environmental Quality (MT DEQ). 2017. Finding of no significant impact: Anaconda-Deer Lodge county wastewater treatment plant improvements. MT DEQ Water Quality Division. Helena, MT.
- Montana Natural Heritage Program (MT NHP). 2018. Montana wetland and riparian mapping. Montana State Library Natural Resource Information System. Missoula, MT.
<http://mtnhp.org/mapviewer/?t=8>.
- Montana Natural Resource Damage Program (MT NRDP). 2007. Draft conceptual Smelter Hill are uplands resources restoration plan. Prepared by Montana Department of Justice, Natural Resource Damage Program. Anaconda Smelter NPL Site, Anaconda, Montana.
- Montgomery, D. R. 1999. Process Domains and the River Continuum. *Journal of The American Water Resources Association* 35:397–410.
- Mulholland, P. J., A. M. Helton, G. C. Poole, R. O. Hall, S. K. Hamilton, B. J. Peterson, J. L. Tank, L. R. Ashkenas, L. W. Cooper, C. N. Dahm, W. K. Dodds, S. E. G. Findlay, S. V. Gregory, N. B. Grimm, S. L. Johnson, W. H. McDowell, J. L. Meyer, H. M. Valett, J. R. Webster, C. P. Arango, J. J. Beaulieu, M. J. Bernot, A. J. Burgin, C. L. Crenshaw, L. T. Johnson, B. R. Niederlehner, J. M. O'Brien, J. D. Potter, R. W. Sheibley, D. J. Sobota, and S. M. Thomas. 2008. Stream denitrification across biomes and its response to anthropogenic nitrate loading. *Nature* 452:202–205.
- Natural Resources Conservation Service (NRCS). 2018. Web Soil Survey. Retrieved from: <https://websoilsurvey.sc.egov.usda.gov/>. Accessed 2/22/18.

- Newbold, J. D., J. W. Elwood, R. V. O'Neill, and W. Van Winkle. 1981. Measuring nutrient spiralling in Streams. *Canadian Journal of Fisheries and Aquatic Sciences* 38:860–863.
- Nidzieko, N. J., J. A. Needoba, S. G. Monismith, and K. S. Johnson. 2014. Fortnightly tidal modulations affect net community production in a mesotidal estuary. *Estuaries and Coasts* 37:91–110.
- Ocampo, C. J., C. E. Oldham, and M. Sivapalan. 2006. Nitrate attenuation in agricultural catchments: Shifting balances between transport and reaction. *Water Resources Research* 42:1–16.
- Palmer, H., M. Beutel, and S. Gebremariam. 2009. High rates of ammonia removal in experimental oxygen-activated nitrification wetland mesocosms. *Journal of Environmental Engineering* 135:972–979.
- Peipoch, M., E. Gacia, E. Bastias, A. Serra, L. Proia, M. Ribot, S. N. Merbt, and E. Martí. 2016. Small-Scale heterogeneity of microbial N uptake in streams and its implications at the ecosystem level. *Ecology* 97:1329–1344.
- Pellerin, B. A., W. A. Wolheim, C. S. Hopkinson, W. H. McDowell, M. R. Williams, C. J. Vörösmarty, and M. L. Daley. 2004. Role of wetlands and developed land use on dissolved organic nitrogen concentrations and DON/TDN in northeastern U.S. rivers and streams. *Limnology and Oceanography* 49:910–918.

- Pennino, M. J., S. S. Kaushal, S. N. Murthy, J. D. Blomquist, J. C. Cornwell, and L. A. Harris. 2016. Sources and transformations of anthropogenic nitrogen along an urban river-estuarine continuum. *Biogeosciences* 13:6211–6228.
- Peterson, B. J., W. M. Wollheim, P. J. Mulholland, J. R. Webster, J. L. Meyer, J. L. Tank, E. Martí, W. B. Bowden, H. M. Vallett, A. E. Hershey, W. H. McDowell, W. K. Dodds, S. K. Hamilton, S. Gregory, and D. D. Morrall. 2001. Control of nitrogen export from headwaters by headwater streams. *Science* 292:86–90.
- Poff, N. L., J. D. Olden, D. M. Merritt, and D. M. Pepin. 2007. Homogenization of regional river dynamics by dams and global biodiversity implications. *Proceedings of the National Academy of Sciences* 104:5732–5737.
- Poole, G. C. 2002. Fluvial landscape ecology: addressing uniqueness within the river discontinuum. *Freshwater Biology* 47:641–660.
- Powers, S. M., R. A. Johnson, and E. H. Stanley. 2012. Nutrient retention and the problem of hydrologic disconnection in streams and wetlands. *Ecosystems* 15:435–449.
- QGIS Development Team. 2019. QGIS Geographic Information System. Open Source Geospatial Foundation Project, Chicago, USA. <http://qgis.osgeo.org>.
- R Core Team. 2013. R: A language and environment for statistical computing. R Foundation for Statistical Computing, Vienna, Austria. URL: <http://www.R-project.org/>.

- Raymond, P. A., J. E. Saiers, and W. V. Sobczak. 2016. Hydrological and biogeochemical controls on watershed dissolved organic matter transport: pulse-shunt concept. *Ecology* 97:5–16.
- Renwick, W. H., S. V. Smith, J. D. Bartley, and R. W. Buddemeier. 2005. The role of impoundments in the sediment budget of the conterminous United States. *Geomorphology* 71:99–111.
- Ribot, M., E. Martí, D. von Schiller, F. Sabater, H. Daims, and T. J. Battin. 2012. Nitrogen processing and the role of epilithic biofilms downstream of a wastewater treatment plant. *Freshwater Science* 31:1057–1069.
- Rosgen, D.L. 1994. A classification of natural rivers. *Catena* 22(3): 169-199.
- Shen, X., T. Sun, F. Liu, J. Xu, and A. Pang. 2015. Aquatic metabolism response to the hydrologic alteration in the Yellow River estuary, China. *Journal of Hydrology* 525:42–54.
- Sponseller, R. A., M. Blackburn, M. B. Nilsson, and H. Laudon. 2018. Headwater mires constitute a major source of nitrogen (N) to surface waters in the boreal landscape. *Ecosystems* 21:31–44.
- Stanford, J. A., M. S. Lorang, and F. R. Hauer. 2005. The shifting habitat mosaic of river ecosystems. *SIL Proceedings, 1922-2010* 29:123–136.
- Starry, O. S., H. M. Valett, and M. E. Schreiber. 2005. Nitrification rates in a headwater stream: Influences of seasonal variation in C and N supply. *Journal of the North American Benthological Society* 24:753–768.

- Steinman, A.D., G.A. Lamberti, P.R. Leavitt, and D.G. Uzarski. 2017. Biomass and pigments of benthic algae. Pages 223-240 in F.R. Hauer and G.A. Lamberti, editors. *Methods in stream ecology*. London, United Kingdom.
- Stelzer, R. S. 2015. Yearlong impact of buried organic carbon on nitrate uptake in stream sediments. *Journal of Environmental Quality* 44:1711–1719.
- Stelzer, R. S., J. Heffernan, and G. E. Likens. 2003. The influence of dissolved nutrients and particulate organic matter quality on microbial respiration and biomass in a forest stream. *Freshwater Biology* 48:1925–1937.
- Strauss, E. A., and G. A. Lamberti. 2002. Effect of dissolved organic carbon quality on microbial decomposition and nitrification rates in stream sediments. *Freshwater Biology* 47:65–74.
- Stream Solute Workshop. 1990. Concepts and methods for assessing solute dynamics in stream ecosystems. *Journal of the North American Benthological Society* 9, 95–119.
- Sudoh, R., M. S. Islam, K. Sazawa, T. Okazaki, N. Hata, S. Taguchi, and H. Kuramitz. 2015. Removal of dissolved humic acid from water by coagulation method using polyaluminum chloride (PAC) with calcium carbonate as neutralizer and coagulant aid. *Journal of Environmental Chemical Engineering* 3:770–774.
- Thouin, J. A., W. M. Wollheim, C. J. Vörösmarty, J. M. Jacobs, and W. H. McDowell. 2009. The biogeochemical influences of NO_3^- , dissolved O_2 , and dissolved organic C on stream NO_3^- uptake. *Journal of the North American Benthological Society* 28:894–907.

- Tobias, C. R., S. a. Macko, I. C. Anderson, E. a. Canuel, and J. W. Harvey. 2001. Tracking the fate of a high concentration groundwater nitrate plume through a fringing marsh: A combined groundwater tracer and in situ isotope enrichment study. *Limnology and Oceanography* 46:1977–1989.
- U.S. EPA and CDM Smith. 2004. Draft final site characterization report north Opportunity ground water and surface water area of concern. Anaconda Smelter NPL Site, Anaconda, Montana.
- U.S. EPA and CDM Smith. 2012. Dutchman creek high arsenic area final design report. Anaconda Smelter NPL Site, Anaconda, Montana.
- U.S. EPA. 1993b. Method 350.1: Determination of ammonia nitrogen by semi-automated colorimetry. Environmental Monitoring Systems Laboratory, Office of Research and Development. Cincinnati, OH.
- U.S. EPA. 1993c. Method 353.1, Revision 2.0: Determination of nitrate-nitrite nitrogen by automated colorimetry. Environmental Monitoring Systems Laboratory, Office of Research and Development. Cincinnati, OH.
- U.S. EPA. 1993d. Method 365.1, Revision 2.0: Determination of phosphorus by semi-automated colorimetry. Environmental Monitoring Systems Laboratory, Office of Research and Development. Cincinnati, OH.
- U.S. EPA. 2005. Method 415.3: Measurement of total organic carbon, dissolved organic carbon, and specific UV absorbance at 254nm in source water and drinking water.

Environmental Monitoring Systems Laboratory, Office of Research and Development.
Cincinnati, OH.

U.S. Geological Survey (USGS). 2018. National Water Information System.

https://waterdata.usgs.gov/mt/nwis/uv?site_no=12323850

Valett, H. M., F. R. Hauer, and J. A. Stanford. 2014. Landscape influences on ecosystem function: Local and routing control of oxygen dynamics in a floodplain aquifer. *Ecosystems* 17:195–211.

Valett, H. M., J. A. Morrice, C. N. Dahm, and M. E. Campana. 1996. Parent lithology, surface-groundwater exchange, and nitrate uptake in headwater streams. *Limnology and Oceanography* 41:333–345.

Valett, H.M. and M. Peipoch. 2018. Nutrient challenges to ecological restoration of the upper Clark Fork River. Report to the Natural Resource Damage Program, Montana Department of Justice. pp. 38.fs

Vannote, R. L., G. W. Minshall, K. W. Cummins, J. Sedell, and C. E. Cushing. 1980. The river continuum concept. *Canadian Journal of Fisheries and Aquatic Sciences* 37:130–137.

Vidon, P., C. Allan, D. Burns, T. P. Duval, N. Gurwick, S. Inamdar, R. Lowrance, J. Okay, D. Scott, and S. Sebestyen. 2010. Hot spots and hot moments in riparian zones: Potential for improved water quality management. *Journal of the American Water Resources Association* 46:278–298.

- Vitousek, P. M., J. R. Gosz, C. C. Grier, J. M. Melillo, W.A. Reiners, and R. L. Todd. 1979. Nitrate losses from disturbed ecosystems. *Science* 204:469–474.
- Walter, R. C., and D. J. Merritts. 2008. Natural streams and the legacy of water-powered mills. *Science* 319:299–304.
- Ward, J.V. and J. Stanford. 1983. The Serial Discontinuity Concept of Lotic Ecosystems. Pages 29-42 in T.D. Fontaine and S.M. Bartell, editors. *Dynamics of Lotic Ecosystems*. Ann Arbor Science, Ann Arbor, Michigan, USA.
- Webster, J. R., P. J. Mulholland, J. L. Tank, H. M. Valett, W. K. Dodds, B. J. Peterson, W. B. Bowden, C. N. Dahm, S. Findlay, S. V. Gregory, and Others. 2003. Factors affecting ammonium uptake in streams—an inter-biome perspective. *Freshwater Biology* 48:1329–1352.
- Wolf, K. L., G. B. Noe, and C. Ahn. 2013. Hydrologic connectivity to streams increases nitrogen and phosphorus inputs and cycling in soils of created and natural floodplain wetlands. *Journal of Environment Quality* 42:1245.
- Wollheim, W. M., T. K. Harms, B. J. Peterson, K. Morkeski, C. S. Hopkinson, R. J. Stewart, M. N. Gooseff, and M. A. Briggs. 2014. Nitrate uptake dynamics of surface transient storage in stream channels and fluvial wetlands. *Biogeochemistry* 120:239–257.
- Zarnetske, J. P., R. Haggerty, S. M. Wondzell, and M. A. Baker. 2011. Dynamics of nitrate production and removal as a function of residence time in the hyporheic zone. *Journal of Geophysical Research: Biogeosciences* 116:1–12.

Zarnetske, J. P., R. Haggerty, S. M. Wondzell, V. A. Bokil, and R. González-Pinzón. 2012.

Coupled transport and reaction kinetics control the nitrate source-sink function of hyporheic zones. *Water Resources Research* 48:1–15.

Table 1. Physicochemical, hydrologic, biogeochemical, and biological parameters by reach over the period of May to September. Data are mean \pm standard error. Values within a row with unique superscripts are statistically different following significant ANOVA (P -value provided) and Tukey's HSD. † denotes log-transformation to meet normality assumptions.

	Reach I	Reach II	Reach III	Reach IV	P -value
<u>Physicochemical</u>					
Dissolved Oxygen (mg L ⁻¹)	10.9 \pm 1.2	10.3 \pm 1.0	9.1 \pm 0.7	8.7 \pm 0.8	0.36
Dissolved Oxygen (% sat.)	122.4 \pm 15.6	117.1 \pm 13.2	103.5 \pm 9.0	99.4 \pm 9.0	0.49
Temperature (°C)	12.2 ^b \pm 1.0	13.48 ^{ab} \pm 0.8	14.5 ^{ab} \pm 0.7	15.2 ^a \pm 0.7	0.047
Sp. Conduct. (μ S cm ⁻¹)	349.5 ^c \pm 17.1	451.2 ^a \pm 25.4	556.9 ^b \pm 24.4	557.7 ^b \pm 22.4	< 0.001
pH	8.6 \pm 0.1	8.6 \pm 0.1	8.6 \pm 0.1	8.6 \pm 0.1	0.98
<u>Hydrologic</u>					
Median Travel Time† (hours)	63.9 ^b \pm 16.1	7.0 ^a \pm 1.1	4.8 ^a \pm 0.4	4.8 ^a \pm 0.9	< 0.001
Q _{up} † (L sec ⁻¹)	841.5 \pm 213.8	664.6 \pm 170.8	1,153.5 \pm 283.5	1,092.0 \pm 334.5	0.56
Q _{in} † (L sec ⁻¹)	327.0 \pm 27.8	NA	NA	NA	NA
Q _{out} † (L sec ⁻¹)	681.5 \pm 121.0	208.7 \pm 31.6	338.1 \pm 83.9	NA	NA
Q _{down} † (L sec ⁻¹)	664.6 \pm 170.8	1,153.5 \pm 283.5	1,092.0 \pm 334.5	1,111.09 \pm 295.9	0.67
Q _{gw} (L sec ⁻¹)	177.7 ^b \pm 107.6	697.6 ^a \pm 138.2	239.03 ^b \pm 87.1	19.1 ^b \pm 80.5	< 0.001
<u>Biogeochemical</u>					
NO ₃ -N (mg L ⁻¹)	0.15 \pm 0.02	0.21 \pm 0.03	0.21 \pm 0.03	0.12 \pm 0.04	0.084
NH ₄ -N† (mg L ⁻¹)	0.01 \pm 0.002	0.01 \pm 0.002	0.01 \pm 0.003	0.02 \pm 0.003	0.51
SRP† (mg L ⁻¹)	0.02 \pm 0.003	0.02 \pm 0.003	0.02 \pm 0.006	0.02 \pm 0.006	0.99
DOC† (mg L ⁻¹)	2.36 \pm 0.33	2.54 \pm 0.39	3.02 \pm 0.64	3.71 \pm 0.76	0.49
<u>Biological</u>					
Chl-a (mg m ⁻²)†	637.4 ^b \pm 342.3	428.1 ^a \pm 148.3	358.8 ^a \pm 97.1	219.6 ^a \pm 77.6	0.016
BOM (g AFDM m ⁻²)†	259.2 ^a \pm 122.8	183.9 ^a \pm 50.6	305.4 ^{ab} \pm 72.0	190.4 ^b \pm 61.6	< 0.001
% Organic Matter†	23.5 ^a \pm 2.6	48.5 ^{ab} \pm 13.7	32.5 ^{ab} \pm 6.6	29.5 ^b \pm 9.6	< 0.05
Autotrophic Index† (mg Chl-a : g AFDM)	1.7 \pm 0.2	2.3 \pm 0.8	1.4 \pm 0.5	1.1 \pm 0.2	0.54

Notes: NA = not applicable due to a lack of replication

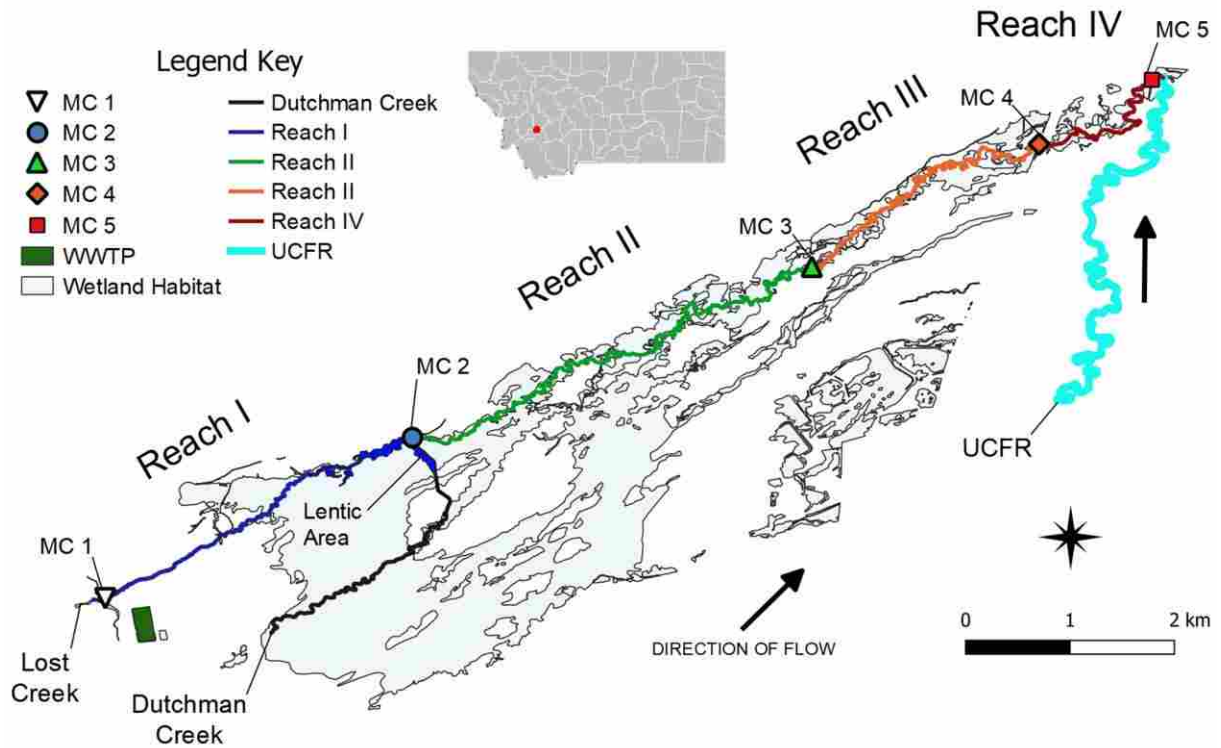


Figure 1. The Lost Creek Dutchman Complex (LCDC) and designated study reaches near Anaconda, MT, USA. Wetland habitat (grey) was identified using geospatial data from the MT Natural Heritage Program. Stream reaches (colored lines) and main-channel sampling sites (MC, colored symbols) are depicted across the four study reaches. Secondary municipal wastewater treatment ponds (WWTP, green polygon) are located near MC 1 at the top of the complex. Dutchman Creek (black) enters Lost Creek through the lentic area (navy blue) at the end of Reach I. In general, water flows from the southwest to the northeast, where Lost Creek converges with the UCFR (teal).

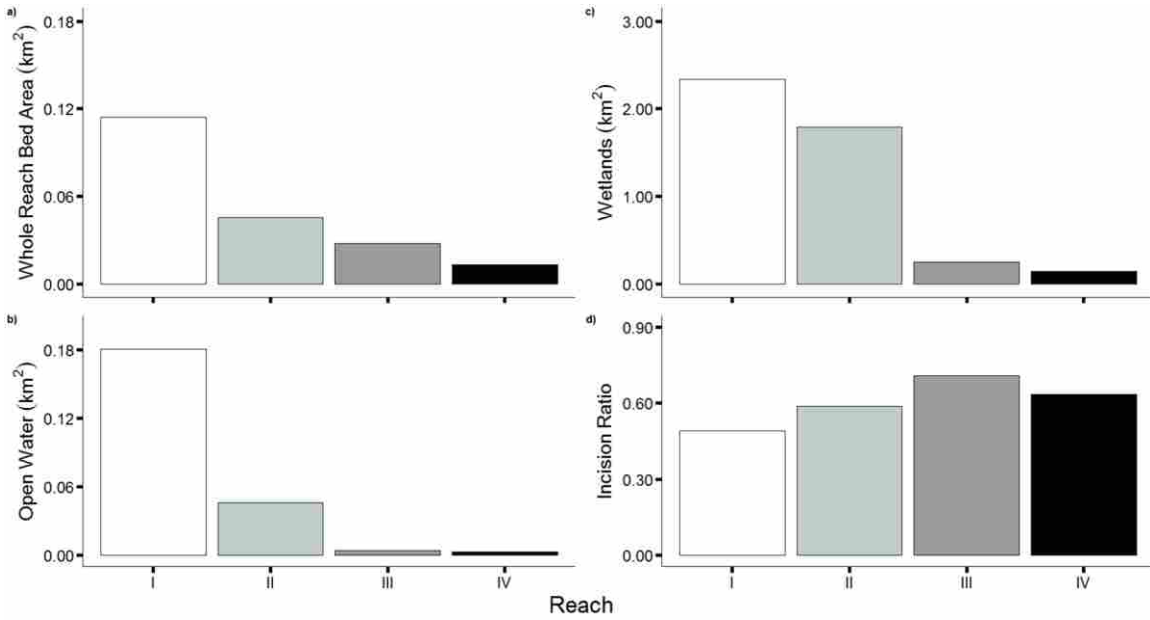


Figure 2. Landscape attributes of the LCDC: (a) whole-reach bed area (km²), (b) open water (km²), (c) floodplain wetlands (km²), and (d) incision ratio of the stream channel by reach. Data demonstrates the transition from wetland-dominated upstream reaches to more incised, downstream lotic channels.

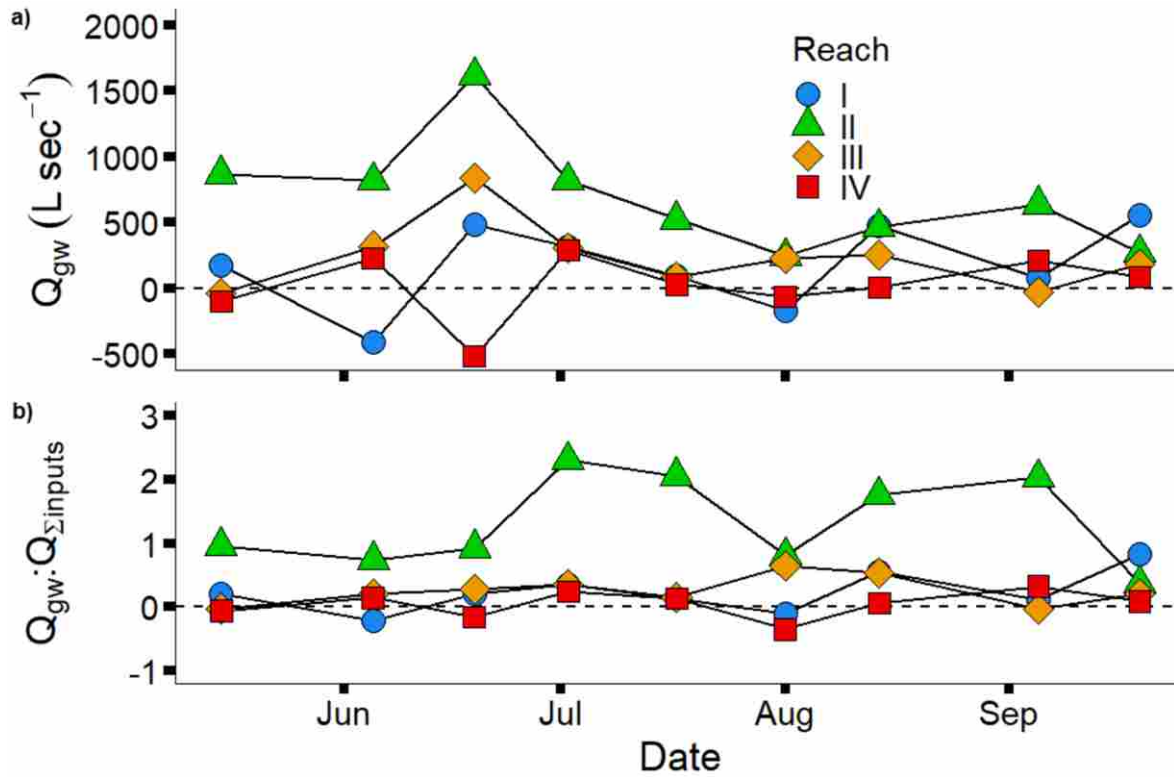


Figure 3. Net groundwater exchange (a) and groundwater exchange as a proportion of total surfacewater inputs (b) for each of the four reaches from May to September. Net groundwater discharge is represented as Q_{gw} values > 0 , whereas $Q_{gw} < 0$ represents net groundwater recharge.

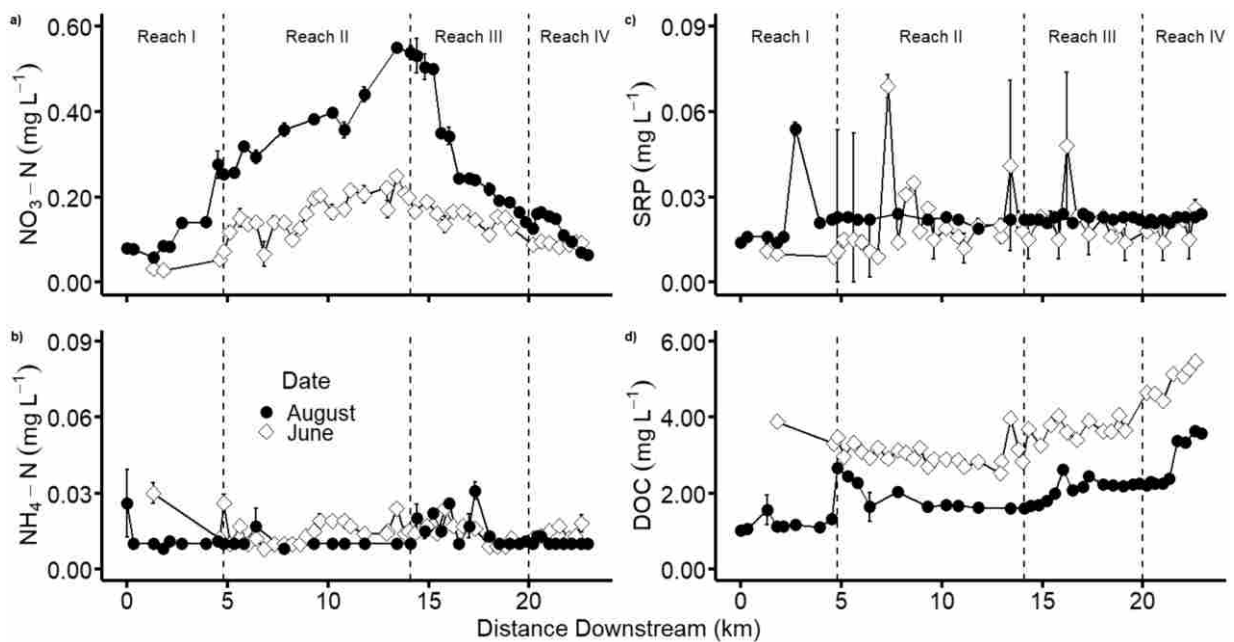


Figure 4. NO_3^- (a), NH_4^+ (b), SRP (c) and DOC (d) concentrations (mean \pm standard error, $n = 3$) on a longitudinal gradient over the course of the entire LCDC during peak (June; white diamonds) and base flows (August; black circles). Dashed vertical lines distinguish study reaches.

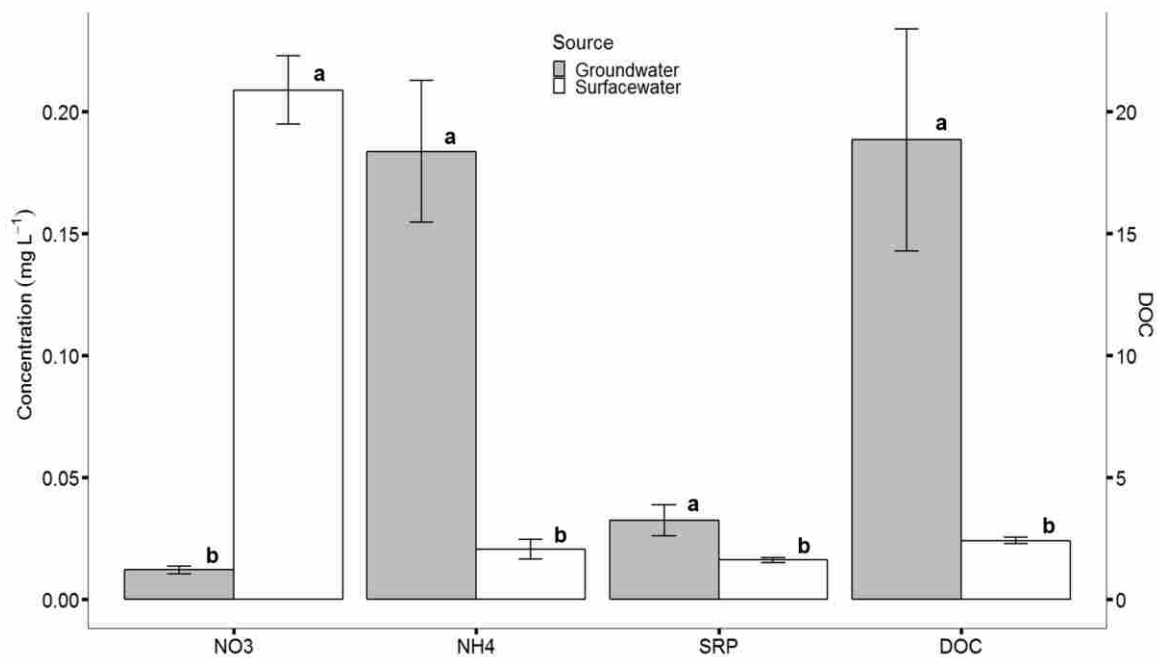


Figure 5. Groundwater (grey) compared to surface water (white) NO₃⁻, NH₄⁺, SRP, and DOC concentration from the LCDC over the entire study period. Data represent grand means ± standard error of all water samples taken from the 10 surface water sampling sites and the 19 groundwater wells. Bars corresponding to each constituent with unique superscripts are statistically different following significant ANOVA and Tukey’s HSD tests.

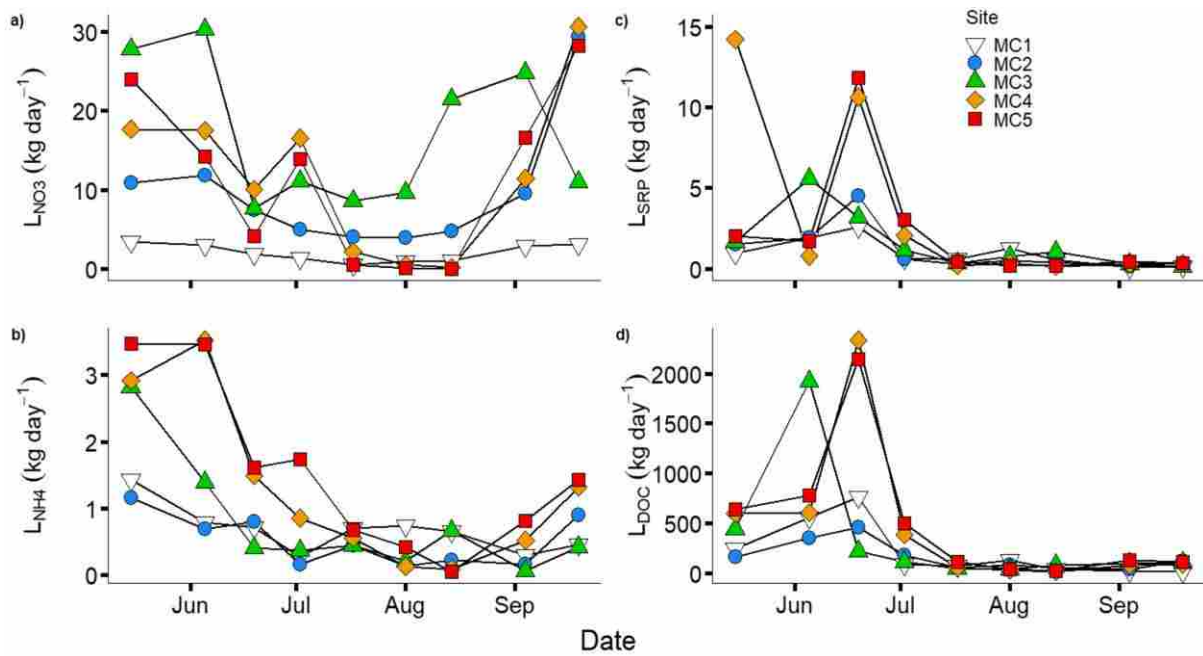


Figure 6. Nutrient loads at each of the five main-channel sites throughout the study period. Data are single values derived from measured stream flow and mean surfacewater concentration on each of nine sampling dates.

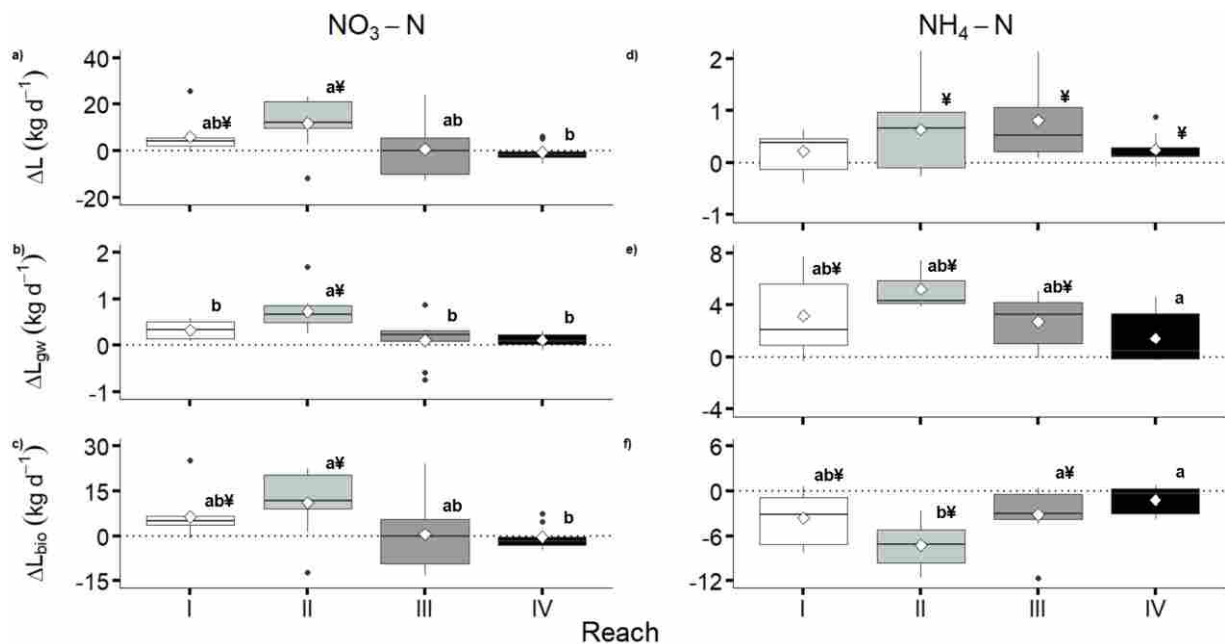


Figure 7. Total change in load (ΔL) partitioned into change in load due to groundwater exchange (ΔL_{gw}) and putative biological processing (ΔL_{bio}) for NO_3^- (a, b, c) and NH_4^+ (d, e, f) by reach. Within each panel, boxplots illustrate distribution and summary statistics: colored boxes represent the 25th to 75th percentiles; center horizontal lines are median values; white diamonds are mean values; whiskers are values in the lowest and highest quartiles that are not significant outliers; black dots are significant outliers, defined as being larger in absolute magnitude than the 25th or 75th percentile minus 1.5-times the interquartile range. Distinct superscripts are reaches that behave differently according to Mann-Whitney U tests, and ¥ represents values that are different from zero according to two-tailed, one-sample Student t-tests.

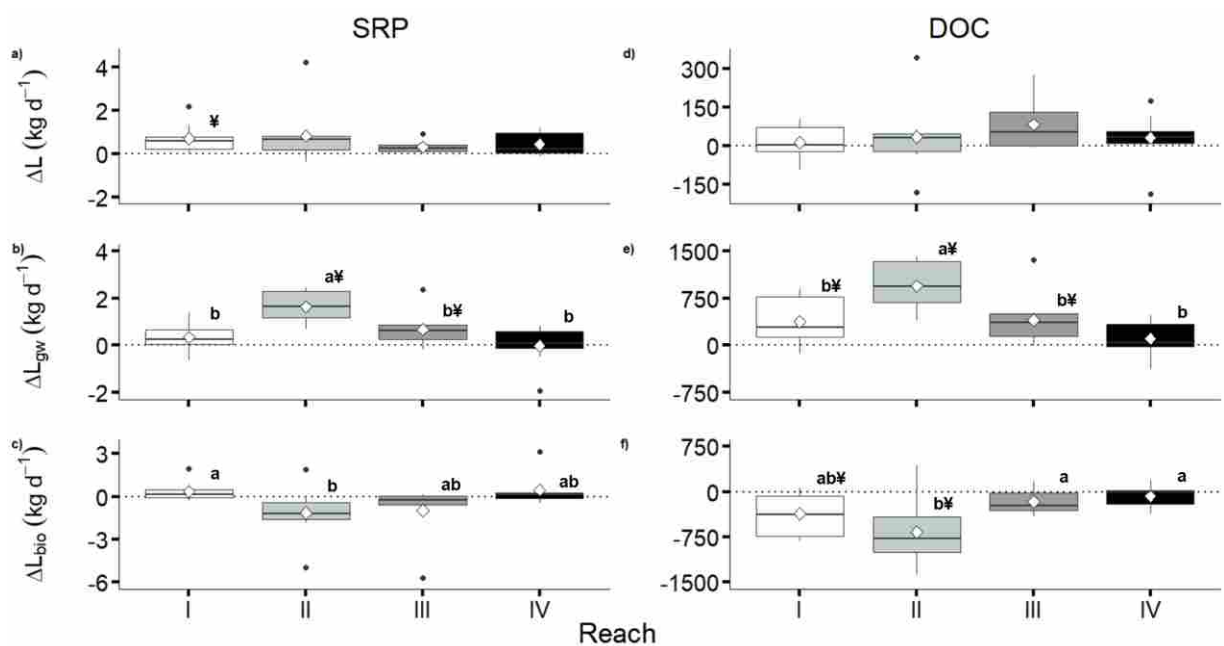


Figure 8. Total change in load (ΔL) partitioned into change in load due to groundwater exchange (ΔL_{gw}) and putative biological processing (ΔL_{bio}) for SRP (a, b, c) and DOC (d, e, f) by reach. Within each panel, boxplots illustrate distribution and summary statistics: colored boxes represent the 25th to 75th percentiles; center horizontal lines are median values; white diamonds are mean values; whiskers are values in the lowest and highest quartiles that are not significant outliers; black dots are significant outliers, defined as being larger in absolute magnitude than the 25th or 75th percentile minus 1.5-times the interquartile range. Distinct superscripts are reaches that behave differently according to Mann-Whitney U tests, and ‡ represents values that are different from zero according to two-tailed, one-sample Student t-tests.

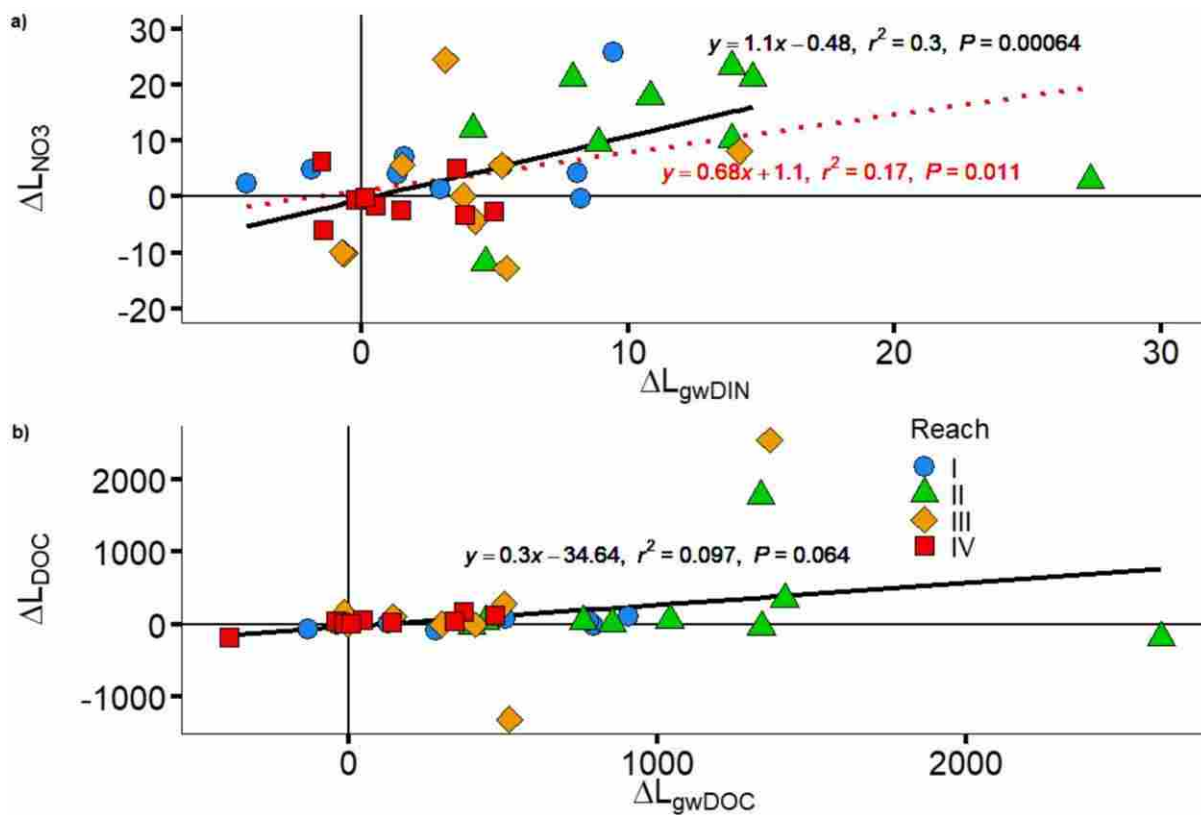


Figure 9. Total measured change in nutrient load (ΔL ; kg d^{-1}) as a function of putative groundwater nutrient load (ΔL_{gw} ; kg d^{-1}). The relationship for total nitrate load change as a function of groundwater DIN exchange (dotted red line) was significant ($r^2 = 0.17$, $P = 0.011$). Exclusion of a single outlier from Reach II (symbol identified by the dashed red circle) improved explanatory power ($r^2 = 0.3$, $P = 0.00064$) and the regression coefficient approached 1 (black solid line). In contrast, ΔL_{DOC} (b) did not exhibit a significant relationship with ΔL_{gwDOC} , suggesting a decoupling of NO_3^- and DOC dynamics at the stream-groundwater interface.

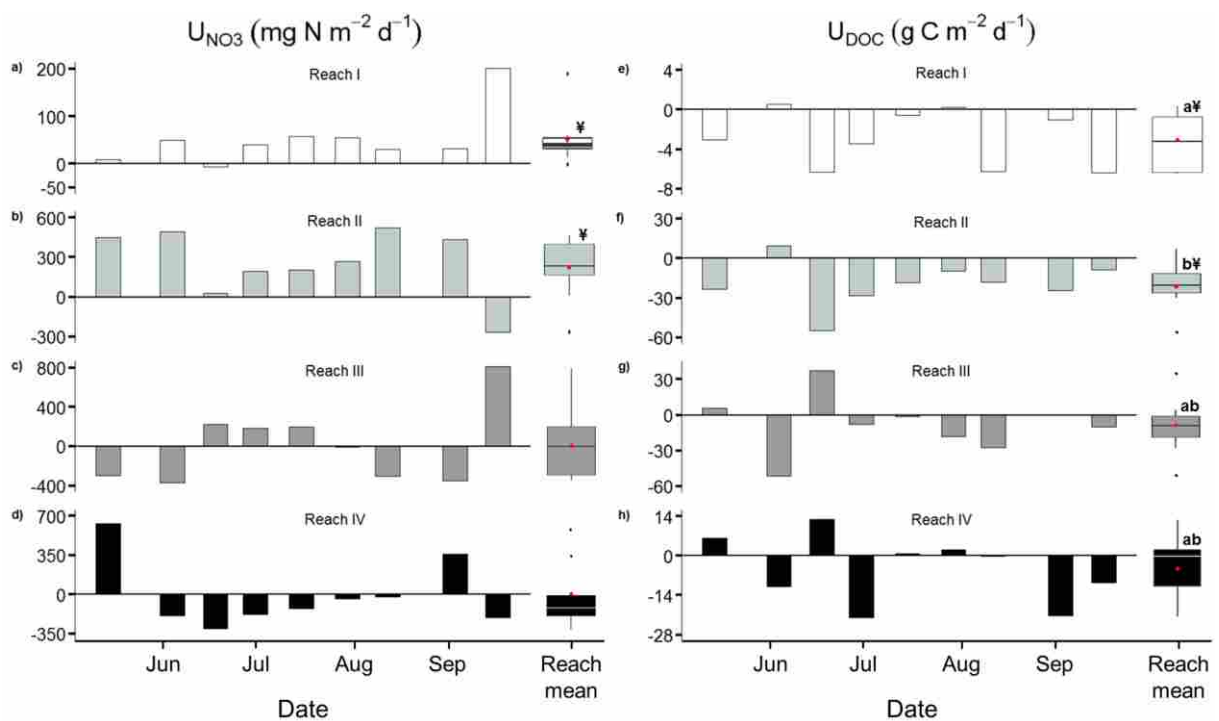


Figure 10. Area-specific biological processing rates (U) of NO_3^- (a, b, c, d) and DOC (e, f, g, h) in the LCDC by reach (colored boxes) and date. Bar plots represent measured rates from nine sampling events. Box plots at the end of the x-axes illustrate distribution and summary statistics for each reach and constituent: colored boxes represent the 25th to 75th percentiles; center horizontal lines are median values; red diamonds are mean values; whiskers are values in the lowest and highest quartiles that are not significant outliers; black dots are significant outliers, defined as being larger in magnitude than the difference between the 25th or 75th percentile and 1.5-times the interquartile range. Distinct superscripts are reaches that behave differently according to Mann-Whitney U tests, and ¥ represents values that are different from zero according to two-tailed, one-sample Student t-tests.

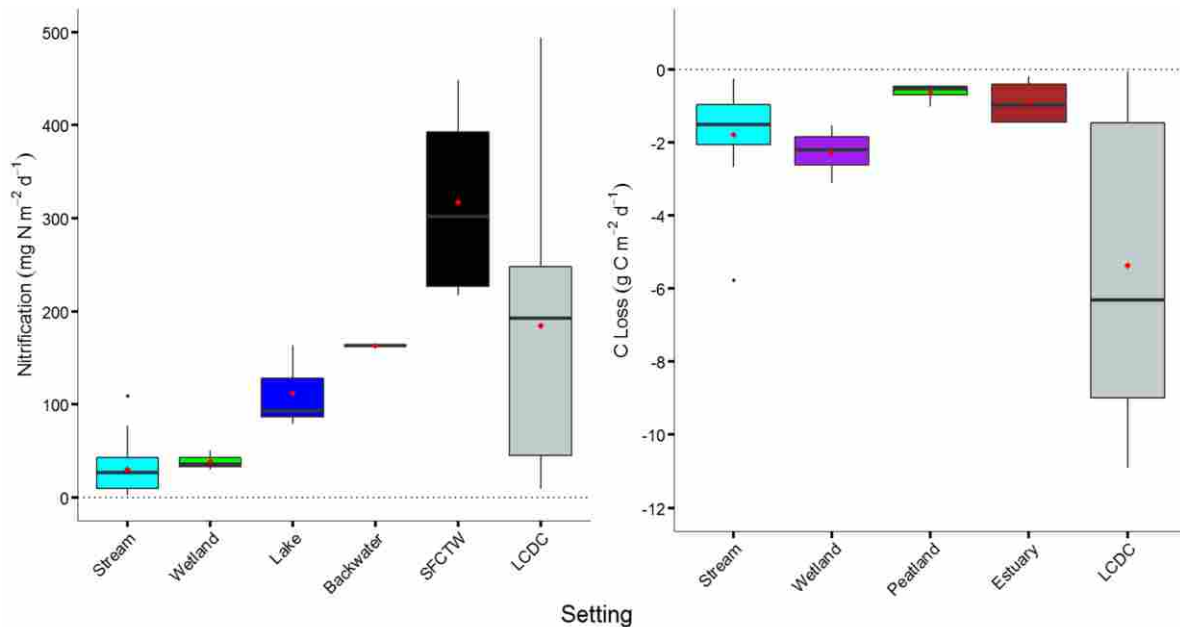


Figure 11. Comparisons between N and C processing rates in the LCDC with those measured in other ecosystems. Boxplots illustrate distribution and summary statistics for each study system setting: colored boxes represent the 25th to 75th percentiles; center horizontal lines are median values; red diamonds are mean values; whiskers are values in the lowest and highest quartiles that are not significant outliers; black dots are significant outliers, defined as being larger in magnitude than the difference between the 25th or 75th percentile and 1.5-times the interquartile range. Nitrification rates were taken from the following studies: *Streams*: Dodds et al. 2000; Starry et al. 2005; Grimm et al. 1991; Brookshire et al. 2005; Straus and Lamberti 2000; Hamilton et al. 2001; Webster et al. 2003. *Wetlands*: Andersen and Hansen 1982; Bowden 1986; Zak and Grigal 1991. *Lake*: Bruesewitz et al. 2012. *Backwater*: Straus et al. 2004. *SFCTW*: Palmer et al. 2009. C Loss rates were taken from the following studies: *Streams*: Fellows et al. 2006; Shen et al. 2015; Meyer and Edwards 1990; Houser et al. 2005; Hamilton et al. 2001; Lupon et al. 2016; Hall et al. 2016. *Wetlands*: Maynard et al. 2012. *Peatlands*: McConnell et al. 2013. *Estuaries*: Hitchcock et al. 2010; Maher et al. 2013; Nidzieko et al. 2014; Caffrey et al. 2014.

Appendix A. Reach, number, name, description, and location of the ten sampling sites.

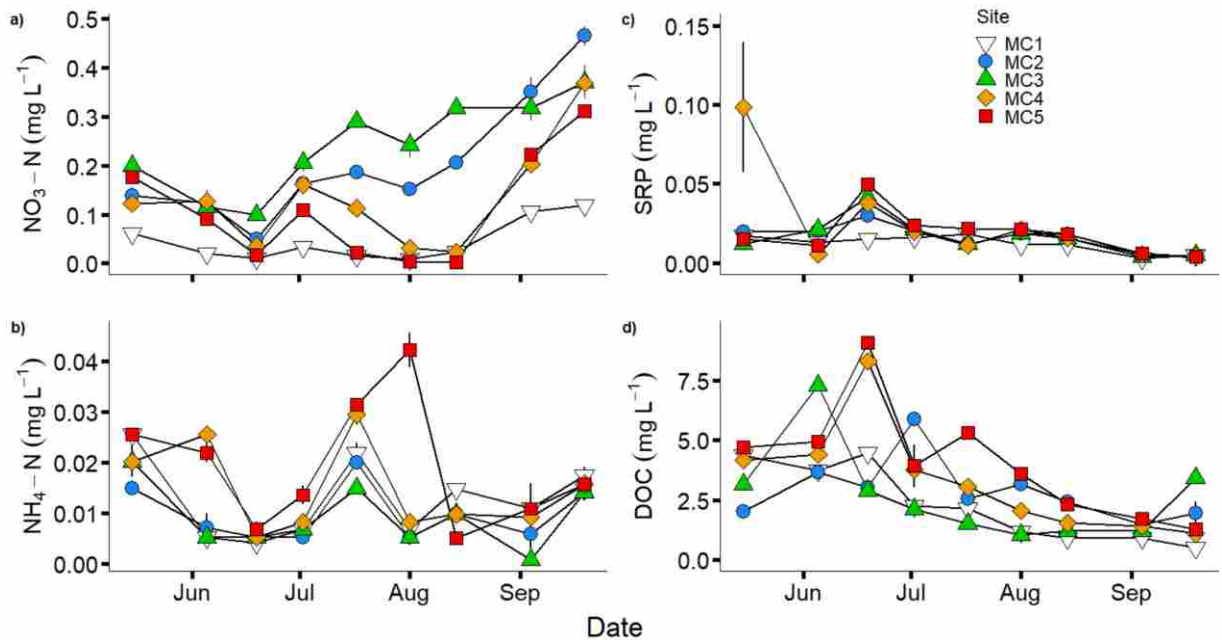
Reach	Site Number	Site Name	Description	Latitude	Longitude
I	MC1	LC-Gardiner	Upstream extent of LCDC; receives mix of Gardiner Ditch and Lost Creek water	46.162388°	-112.889900°
I	OUT1.1	Ueland Ranch Ditch	Diversion ditch on Ueland Ranch removes Lost Creek water from channel	46.170770°	-112.874364°
I	IN1	Dutchman Creek	At south end of Dutchman Dyke where Dutchman Creek is diverted into reservoir	46.176138°	-112.848678°
I	OUT1.2	Fifer-Cummock Ditch	Diversion ditch removes water from reservoir	46.182764°	-112.851649°
I/II	MC2	Dutchman Dyke	Flow control structure regulates outflow from reservoir into reach II of LCDC	46.182322°	-112.851795°
II	OUT2	Jacobson Ditch	Diversion ditch removes Lost Creek water from channel	46.202907°	-112.805709°
II/III	MC3	Heggelund Crossing	Lost Creek bridge crossing on Heggelund Ranch	46.203490°	-112.802260°
III	OUT3	Beckstead Ditch	Diversion ditch removes Lost Creek water from channel	46.206248°	-112.799093°
III/IV	MC4	USGS downstream	Gage station 12323850 Lost Cr near Galen on Frontage Rd.	46.218687°	-112.774075°
IV	MC5	Confluence	Lost Creek bridge crossing on Lambert Ranch near confluence of Lost Creek and UCFR	46.226652°	-112.760091°

Notes: Sites with multiple roman numeral identifiers were used as both upstream and downstream extents for linked reaches.

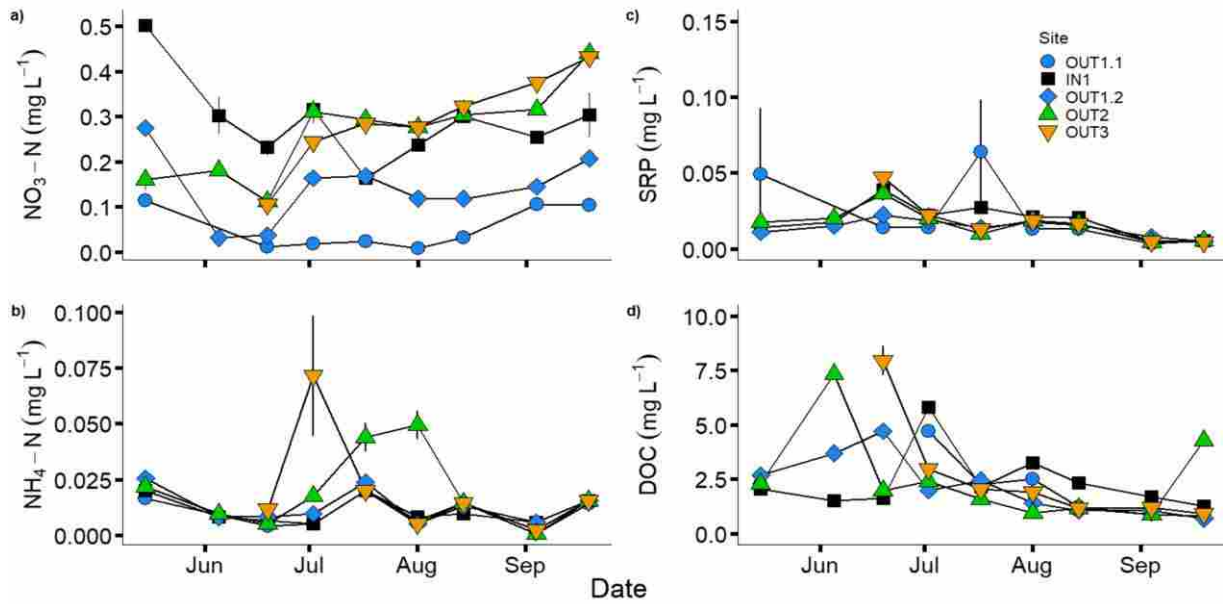
Appendix B. Geomorphic parameters and landscape attributes by reach. Data are means \pm standard errors. Values with unique superscripts are statistically different following Tukey's HSD. † denotes log-transformation to meet normality assumptions.

	Reach I	Reach II	Reach III	Reach IV	<i>p</i> -value
Bankfull Width (m) [†]	5.87 \pm 0.99	5.20 \pm 0.38	5.40 \pm 0.35	4.83 \pm 0.28	0.92
Channel Length (m)	4805	9341	6163	2824	NA
Bankfull Depth (m)	0.55 ^b \pm 0.01	0.64 ^a \pm 0.02	0.59 ^{ab} \pm 0.02	0.81 ^c \pm 0.02	< 0.001
Mean Bankfull Depth (m) [†]	0.55 ^a \pm 0.03	0.64 ^a \pm 0.04	0.59 ^a \pm 0.04	0.81 ^b \pm 0.04	< 0.001
Max Bankfull Depth (m)	0.68 ^b \pm 0.05	0.86 ^a \pm 0.05	0.80 ^{ab} \pm 0.05	0.93 ^a \pm 0.05	0.0073
Incision Ratio	0.49 ^b \pm 0.05	0.59 ^{ab} \pm 0.04	0.73 ^a \pm 0.03	0.75 ^a \pm 0.06	< 0.001
Width:Depth [†]	11.51 \pm 2.22	9.65 \pm 1.45	9.71 \pm 1.05	6.23 \pm 0.60	0.11
Low Bank Height (m)	0.34 ^c \pm 0.04	0.52 ^a \pm 0.04	0.58 ^{ab} \pm 0.04	0.72 ^b \pm 0.08	< 0.001
Cross-sectional Area (m ²)	3.15 \pm 0.51	3.21 \pm 0.32	3.12 \pm 0.19	3.88 \pm 0.25	0.112
Pool Width (m)	3.12 \pm 0.84	1.57 \pm 0.49	4.50 \pm 0.61	4.27 \pm 1.19	NA
Pool Depth (m)	0.62 \pm 0.17	0.47 \pm 0.14	0.65 \pm 0.11	1.15 \pm 0.20	NA
Pool Width:Depth [†]	7.71 \pm 3.87	3.38 \pm 0.38	7.99 \pm 1.85	4.01 \pm 1.28	0.23
Riffle Length (m)	15.60 ^b \pm 3.04	22.30 ^{ab} \pm 4.19	16.01 ^{ab} \pm 3.02	28.71 ^a \pm 2.40	0.018
Run Length (m) [†]	14.67 ^b \pm 2.26	19.29 ^{ab} \pm 2.46	35.52 ^b \pm 12.19	29.12 ^{ab} \pm 6.08	0.040
Riffle:Run	1.06	0.22	0.38	1.38	NA
Debris Dams (m ³)	5.06 ^b \pm 1.55	0.18 ^a \pm 0.18	5.20 ^{ab} \pm 4.16	1.32 ^{ab} \pm 0.12	0.015
Number of Channels [†]	1.25 \pm 0.10	1.14 \pm 0.10	1.17 \pm 0.11	1.08 \pm 0.08	0.61
Open Water (km ²)	0.18	0.046	0.004	0.0028	NA
Floodplain wetland (km ²)	2.34	1.79	0.25	0.15	NA
Upland (km ²)	4.17	3.62	1.04	0.32	NA
Percent Wetland (%)	34.93	32.78	19.35	31.92	NA
Percent Open Water (%)	2.70	0.84	0.32	0.61	NA
Sinuosity	1.23	2.06	2.19	1.80	NA
Whole-Reach Bed Area (km ²)	0.11 ^a \pm 0.01	0.045 ^b \pm 0.0011	0.028 ^c \pm 0.0022	0.013 ^d \pm 0.00094	< 0.001

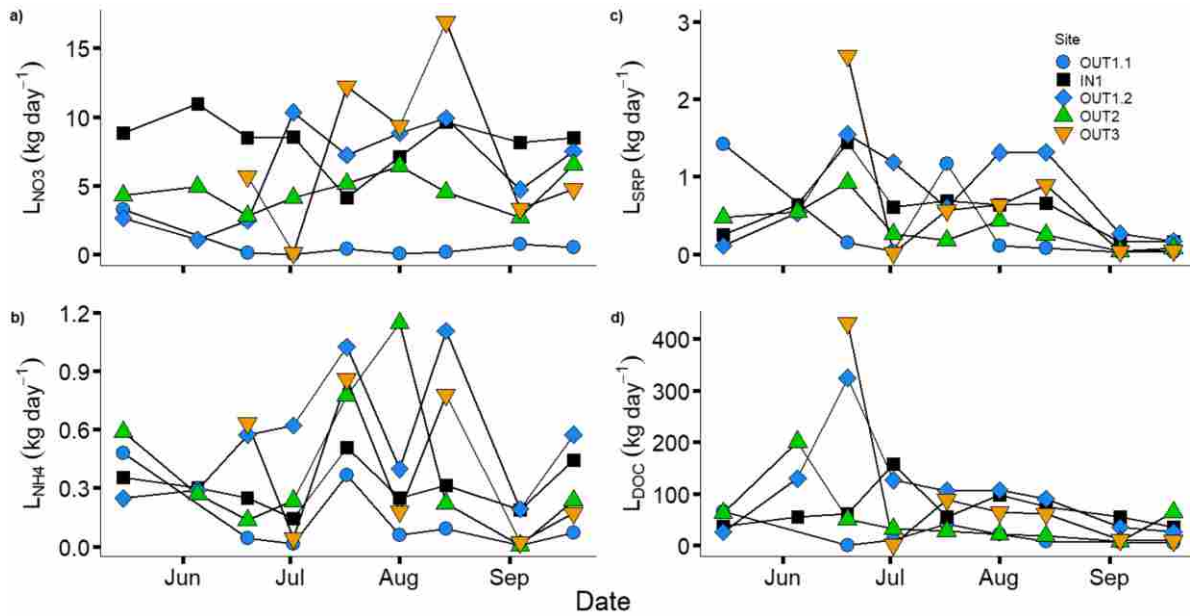
Notes: NA values are due to a lack of replicate measurements.



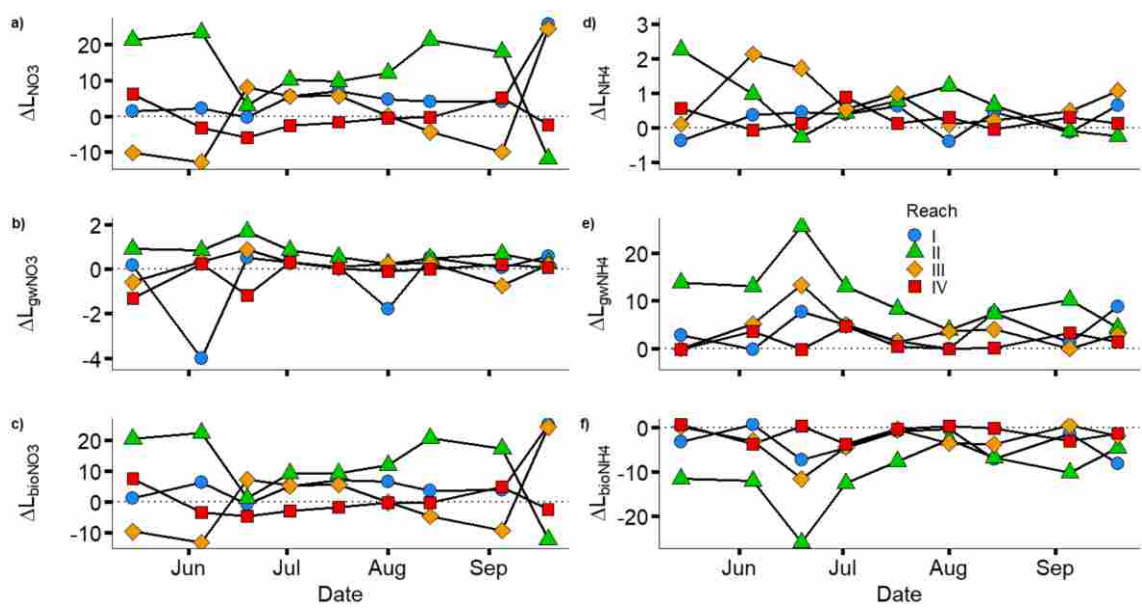
Appendix C. Nutrient concentration (mean \pm SE) of each of the dissolved constituents at the five main-channel sites throughout the study period. Across all sites, NO_3^- (a) concentration typically increased as the summer progressed. (b) NH_4^+ concentration was diluted during high flow and peaked in mid-summer. (c) SRP remained low and relatively stable throughout the summer period, but increased slightly during peak flood. (d) DOC increased with spring runoff and continued to decline as the summer progressed.



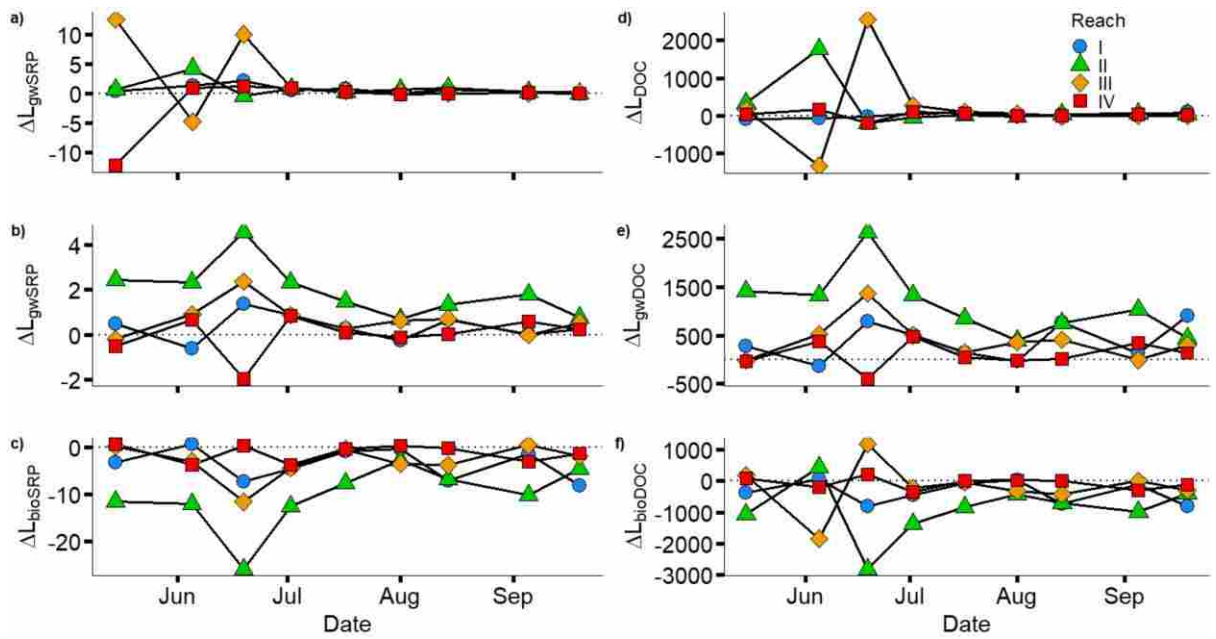
Appendix D. Nutrient concentration (mean \pm SE) of each of the dissolved constituents at the five irrigation ditches/tributary inputs throughout the study period. Colors represent reach designation (blue = Reach I; black = Dutchman Creek tributary; green = Reach II; orange = Reach III) and identification scheme represents direction of flow and position along the sequence (i.e., OUT1.1 = outflow, Reach I, site 1).



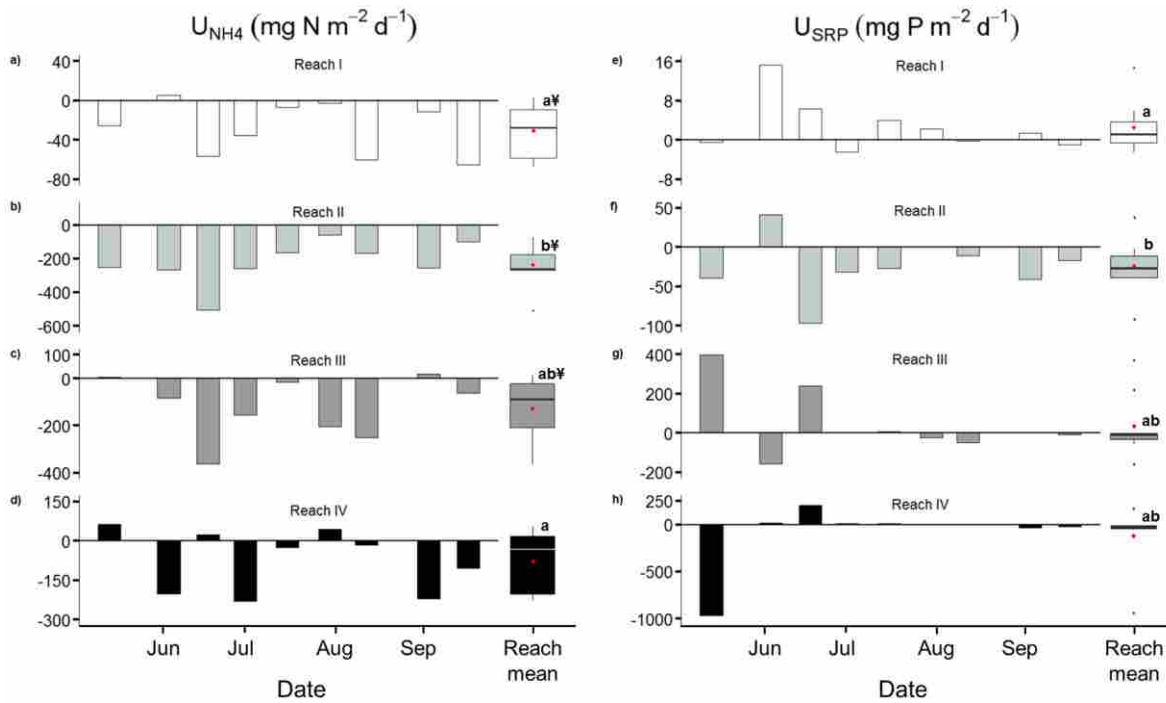
Appendix E. Loads of each of the dissolved constituents at the five irrigation ditches/tributary inputs throughout the study period. Data are single values derived from measured stream flow and mean surfacewater concentration on each of nine sampling dates. Colors represent reach designation (blue = Reach I; black = Dutchman Creek tributary; green = Reach II; orange = Reach III) and identification scheme represents direction of flow and position along the sequence (i.e., OUT1.1 = outflow, Reach I, ditch 1).



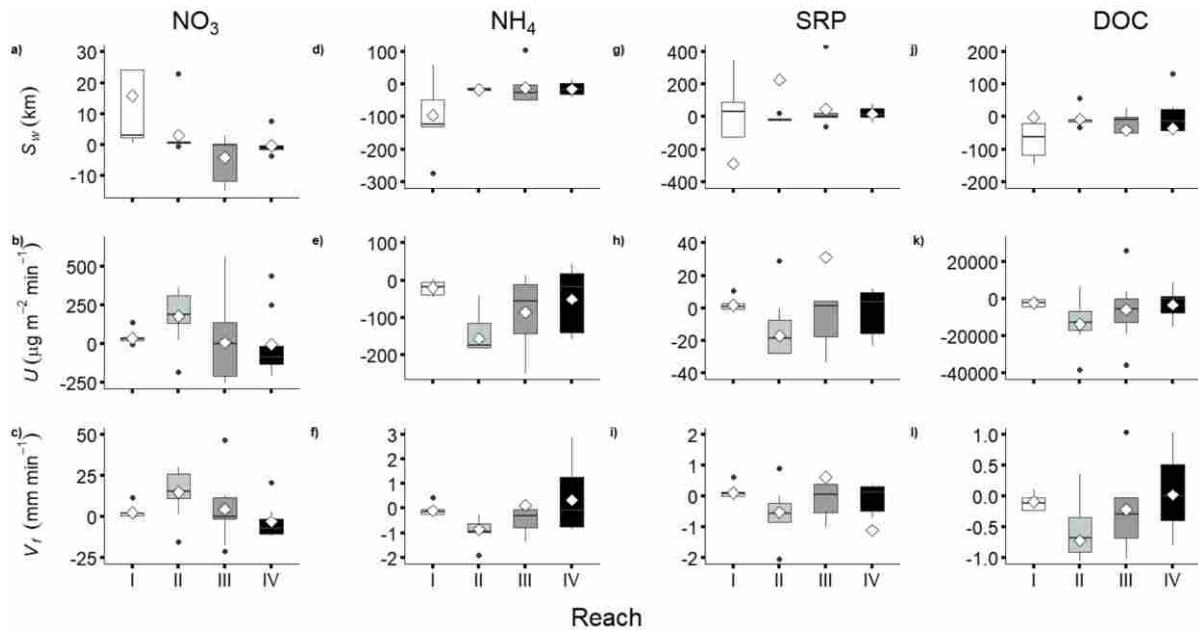
Appendix F. Total changes in load (ΔL), estimated groundwater loads (ΔL_{gw}), and biologically-driven changes in load (ΔL_{bio}) for NO_3^- (a, b, c) and NH_4^+ (d, e, f) by reach and date.



Appendix G. Total changes in load (ΔL), estimated groundwater loads (L_{gw}), and biologically-driven changes in load (L_{bio}) for SRP (a, b, c) and DOC (d, e, f) by reach and date.



Appendix H. Area-specific biological processing rates (U) of NH_4^+ (a, b, c, d) and SRP (e, f, g, h) in the LCDC by reach (colored boxes) and date. Bar plots represent measured rates from nine sampling events. Box plots at the end of the x-axes illustrate distribution and summary statistics for each reach and constituent: colored boxes represent the 25th to 75th percentiles; center horizontal lines are median values; red diamonds are mean values; whiskers are values in the lowest and highest quartiles that are not significant outliers; black dots are significant outliers, defined as being larger in magnitude than the difference between the 25th or 75th percentile and 1.5-times the interquartile range. Distinct superscripts are reaches that behave differently according to Mann-Whitney U tests, and # represents values that are different from zero according to two-tailed, one-sample Student t-tests.



Appendix I. Uptake length, uptake rate, and uptake velocity for each dissolved nutrient by reach.

$$\text{Eq. 5: } V_f = \frac{U}{C}$$

$$\text{Eq. 6: } S_w = \frac{Q}{wV_f}$$

Eq. 5 states that uptake velocity (V_f ; m d^{-1}) is U divided by the average nutrient concentration (C , mg m^{-3}) for each reach and sampling date. Uptake length (S_w ; m) is Q divided by the product of stream width and V_f (Eq. 6). Processing efficiency (ϵ ; %; Eq. 7), is calculated as ΔL_{bio} divided by total surfacewater inputs ($L_{\Sigma\text{inputs}}$; upstream + tributary inflows) multiplied by 100 to derive percent removal or production. For literature comparisons, U is reported in $\mu\text{g m}^{-2} \text{min}^{-1}$, V_f in mm min^{-1} , and S_w in km . We report both positive and negative values of all spiralling metrics to reflect losses (-) and gains (+) to surfacewater and address potential mechanisms of solute processing among groundwater, benthic, and surfacewater compartments.